THE MODELING AND OPTIMIZATION OF 802.11P VANETS UNICAST PERFORMANCE

XIE YU

M.Phil

The Hong Kong Polytechnic University

2017

The Hong Kong Polytechnic University

Department of Electronic and Information Engineering

The Modeling and Optimization of 802.11p VANETs Unicast Performance

XIE YU

A thesis submitted in partial fulfilment of the requirements for the degree of Master of Philosophy

October 2016

CERTIFICATE OF ORIGINALITY

I hereby declare that this thesis is my own work and that, to the best of my knowledge and belief, it reproduces no material previously published or written, nor material that has been accepted for the award of any other degree or diploma, except where due acknowledgement has been made in the text.

____ (Signed)

_______________XIE YU______________(Name of student)

Abstract

802.11p vehicular ad-hoc networks (VANETs) are drawing growing research attentions, as it will play an important role in future Intelligent Transportation Systems (ITS) for ubiquitous communications and connectivity of vehicles. Various messages can be transmitted in a VANET to improve road safety and furnish multiple types of application services. Therefore, the evaluation of VANET performance and its optimization should be indispensably considered. Previous conventional considerations of pertinent studies on VANET modeling did not take a realistic vehicular traffic distribution into account. They merely incorporated a general homogeneous road scenario. Furthermore, most of previous works primarily focused on the broadcasting performance in VANETs, since the safety beacon packets, which were crucial for reducing traffic accidents, were transmitted in periodic broadcast. However, with respect to certain service data (e.g., sensor data), unicast with the re-transmission mechanism is more appropriate, as it aims to ensure successful reception of data. Considering the prospective integration of VANET with the mobile Internet, unicast should also be brought to the forefront. On the other hand, most of the VANET optimization schemes amid previous researches required continuous monitoring of the network and measuring the number of neighboring nodes (e.g., through the feedback-loop principle or local neighbor discovery) to configure the transmission power or adjusting the transmission rate accordingly. Such monitoring and measurement led to large transmission overheads and measurement delay. In view of these inadequacies, a set of 802.11p unicast modeling and optimization methodologies without continuous measuring the number of neighbors are proposed under a practical stochastic traffic modeling framework for estimating and optimizing the vehicle-to-vehicle (V2V) network performance in this thesis.

The modeling is composed of four portions: (i) a stochastic traffic model that describes the realistic traffic road with traffic signaling lights and outputs a vehicular density profile based on the empirical velocity profile; (ii) the contention model based on

a two-dimensional Markov chain depicting the 802.11p unicast channel access contention process of each node at different locations on the road with the density profile from the stochastic traffic model; (iii) an interference model which characterizes the interference triggered by concurrent transmissions and hidden nodes to each node in the network with the foregoing density profile; and (iv) the performance model that analyzes the delay and throughput performances for each node at dissimilar locations based on the resultant parameters output from the two foresaid models. In sum, given a velocity profile as the input, the analytical delay and throughput performance can be attained through our modeling. The feasibility of these modeling methodologies has been rigorously verified by extensive simulation. In both the analytical and simulated results for delay and throughput, we found that the signal-controlled stochastic traffic distribution of vehicles inflicts conspicuous impact on the unicast performance, which provides insights into the studies of the interaction between road traffic and communication network performance. The modeling methodologies proposed in this thesis can be utilized to predict network performance, and traffic and network planning can be carried out respectively to further optimize the data delivery in VANETs.

Based on the analytical modeling of 802.11p VANETs performance, state-of-the-art optimization methods are put forward for each node in the network to reduce packet collisions and enhance the overall network performance. For instance, the optimal transmission range and the optimal Medium Access Control (MAC) contention window size at different locations can be derived prior to vehicles' entering the road segment from the established unicast modeling methodology. With the optimal values reaped pre-emptively, vehicles can adjust their relevant performance parameters once they arrive at corresponding locations on the road. The cross-layer proposal in this thesis involves both the physical (PHY) layer controlling the transmission power and the MAC layer controlling the channel access rate, and the optimization schemes are well-evaluated through extensive simulation. Our results indicate that delay (throughput) is improved by about 53% (120%) on average for homogeneous traffic with different density levels and 45% (104%) on average for heterogeneous traffic at all locations through the cross-layer optimization.

External Publications

Part of the contents in the thesis were presented in the following publications:

1. H. J. Qiu, I. W.-H. Ho, C. K. Tse, and Y. Xie, "A Methodology for Studying 802.11p VANET Broadcasting Performance with Practical Vehicle Distribution," *IEEE Transactions on Vehicular Technology*, vol. 64, no. 10, pp. 4756 – 4769, 2015.
2. Y. Xie, I. W.-H. Ho and L. F. Xie, "Stochastic modeling and analysis of unicast performance in 802.11p VANETs," *International Conference on Information, Communications and Signal Processing (ICICS)*, 2015.

Acknowledgements

I am sincerely indebted to my thesis supervisor, Dr. Ivan Wang-Hei Ho for giving me the great, munificent and patient instruction, guidance and advice not only for my postgraduate study but also for life development. His splendid wisdom and erudite knowledge inspired me in research and helped me to overcome difficulties one after another. He also showed me the rigorous and decent presentation for academic articles writing. His excellent professional spirit and work attitude to pursue the high quality deeply impressed me. He always encouraged me when I confronted problems and granted me the brave to reach the end of the tunnel to see the dawn of triumph.

Moreover, I also need to express my great gratitude to Mr. Harry Jian Feng Qiu for his research outcomes as wondrously helpful and valuable references to me. He generously provided his simulated data to support me for establishment of the simulation framework in my research, and proposed precious suggestions concerning my work.

In addition, special appreciation to Dr. Ling Fu Xie for proofreading and revising some parts of my thesis. He also ungrudgingly imparted his research experience to me for accomplishment of the whole thesis writing.

Finally, deeply thanks to my parents for their love and full support spiritually and materially during my study and all they have done throughout my life. I hereby devote this thesis to them.

This work is partially supported by the Early Career Scheme (Project No. 25200714) established under the University Grant Committee of the Hong Kong Special Administrative Region, China, the National Natural Science Foundation of China (NSFC) (Project No. 61401384). The work is also supported by the research studentship awarded from The Hong Kong Polytechnic University (PolyU) and by the NSFC under the PolyU Shenzhen Research Institute.

Table of Contents

List of Figures

List of Tables

Chapter 1 Introduction

1.1 Motivation and Contributions

In the near future, it is expected that there will be three types of vehicles, namely conventional vehicles, connected vehicles and autonomous vehicles. Conventional vehicles can only interact with other drivers through the horns and lighting signals. Drivers still have to pay attention to the road condition and nearby objects by themselves, though telematics systems and applications installed on vehicles for navigation and localization through the cellular network can be employed as assistance. Whereas, connected vehicles equipped with vehicular devices can intelligently transmit various data (safety or non-safety related messages) [1] for interaction with other vehicles and alerting the human drivers. Autonomous vehicle is the most advanced among the three categories. They are not only capable of automatically sensing roads and objects, but also able to infer environments they may confront subsequently. Currently, almost all vehicles are conventional ones primarily supported by cellular network. Nonetheless, connected vehicles have been partially put into use, and sophisticated autonomous vehicles will possibly appear in the market in the near future.

With respect to the latter two types of vehicles, cellular network alone is not sufficient for satisfying the vehicles' communication demand, Vehicular Ad-hoc Networks (VANETs) that enables Vehicle-to-X (V2X) communications should be adopted for reducing the cost and energy consumption. In traditional cellular network, end-to-end communications between mobile users are realized by base stations that are connected to the backbone network. In contrast, VANETs are decentralized networks without relying on external facilities (e.g., base stations, wireless access points) for Vehicle-to-Vehicle (V2V) and Vehicle-to-Infrastructure (V2I) short-range communications. By the virtue of the distributed structure in VANETs with no central controlling nodes, it is very convenient for inter-networking whenever any car joins or leaves the network regions; besides, the network is more robust when suffered from network attacks or unpredictable traffic accidents, in which the remaining nodes can still be normally connected even if one or more nodes are corrupted or damaged. In addition, VANET is more scalable and more flexible, since it can be established as an independent network in absence of any external facilities. Meanwhile, it can also work together with the cellular network in a hybrid manner. In general VANET communications suffer from lower latency and get faster responsive time when compared with traditional cellular network. Moreover, the expenditure on network construction (e.g., deployment of base stations) and communication energy consumption can also be significantly saved through V2X communications. Based on VANET, various safety and non-safety related applications can be deployed to greatly improve road safety and traffic/transportation efficiency [2]. As a result, VANET conforms to the forthcoming innovation of smart transportation much better than traditional cellular network, and is therefore studied in this thesis.

High mobility and the distribution of cars on the road actually affect the performance of VANET. Hence, modeling traffic consistently and practically is critical for the analysis of vehicular networks. Among the previous works, there was a lack of considering vehicular traffic in signalized urban area. Most of them simply assume a homogeneous vehicle distribution for the VANET traffic. Because of this shortcoming, this thesis adopts a stochastic traffic modeling approach complying with the models proposed by Ho et al. [3], which reflects the practical on-road vehicle distribution and considers the effect of traffic lights for VANET traffic modeling.

Moreover, broadcasting in IEEE 802.11p [5] is widely used in road safety and traffic efficiency applications [4] in VANETs. Thus far, a body of earlier works have been devoted to the study of broadcasting performance in VANETs (e.g., [1, 6]). Nevertheless, broadcast has two drawbacks. The first one is the broadcasting storm [7] by rapid change of network topology that a wondrously large number of cars broadcast messages at the same time. This will result in a mass of information packets collisions, and trigger drastic network performance decline. The other disadvantage is that broadcasting is incapable of ensuring the successful transmission without the transmission of acknowledgement (ACK) packets. Thereby, broadcast is inadequate for some non-safety applications with multimedia streams (e.g., infotainment applications [8], sensor data). For these cases, unicast instead of broadcast is more preferable, because unicast employs a retransmission mechanism and confirmation procedure that the ACK packet is sent from the destination node to the source node upon successful reception, which is able to avert the broadcasting storm and assure the successful transmission. Therefore, in this thesis, unicast performance is modeled and evaluated for 802.11p VANET applications.

In addition, performance optimization is another important topic in VANET research, as it can enhance VANET efficiency for various safety services to reduce accidents and application services to promote life convenience. However, a majority of existing algorithms require incessantly monitoring and measuring ambient number of vehicles through control data exchange, which bring about measuring delay and transmission overheads. In consideration of these defects, optimization approaches that investigate the surrounding traffic circumstance while avoiding transmission overheads for measurements are explored in this thesis.

To sum up, the proposed 802.11p VANET unicast models which consists of the stochastic traffic model and the network model are configured for each node at different locations; the performance optimization at every location is conducted based on the vehicular density and performance information provided by the stochastic traffic model and network model respectively. We only focus on V2V communications in this thesis. The overview of the system structure for 802.11p VANET unicast performance joint modeling and optimization is presented as block diagrams in Figure 1.1 below.

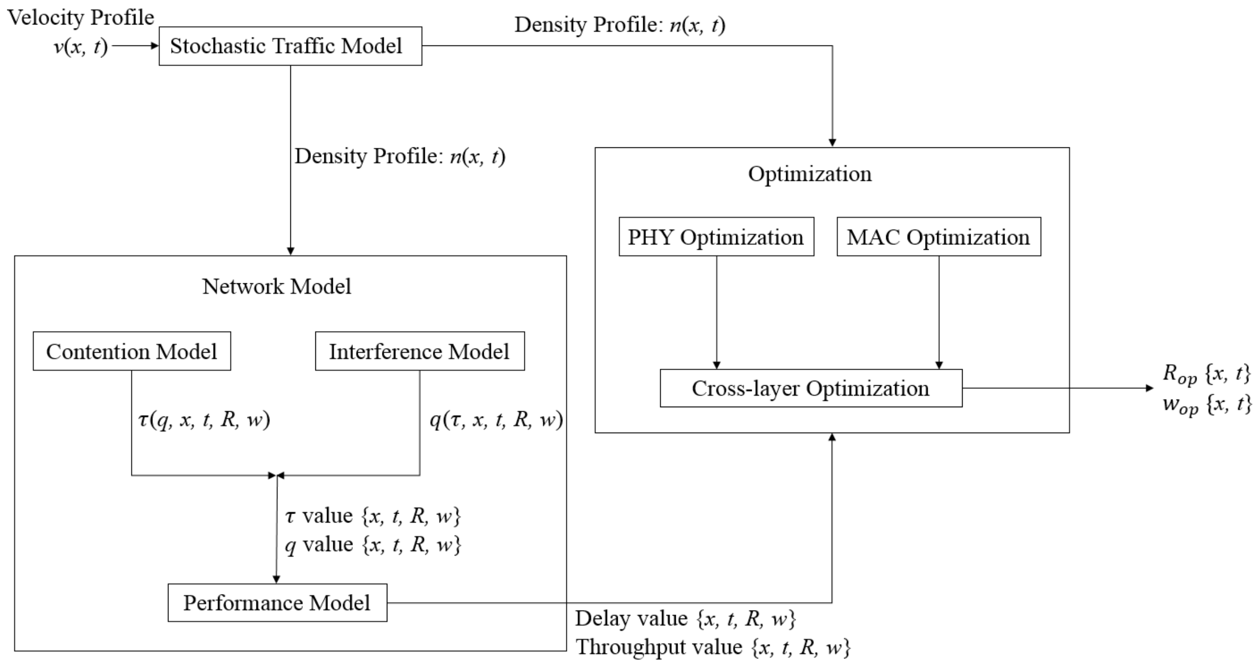

Figure 1.1. Block diagram for the methodology of 802.11p VANET unicast modeling and optimization.

With the velocity profile input, the stochastic traffic model generates a vehicular density profile $n(x,\ t)$ which is a function of location x and time t. The network model comprises three parts: a contention model, an interference model and the performance model. Given the density profile from the stochastic traffic model, the transmission probability expression $\tau(q,\ x,\ t,\ R,\ w)$ of each node can be derived from the contention model. It is a function of collision probability q (caused by other concurrent transmissions or hidden terminals) of a transmission, location, time, and transmission range R, as well as contention window size w for setting the countdown duration of channel access contention on the MAC layer. The interference model outputs the collision probability expression. By combining these two expressions, transmission probability values and collision probability values at different locations, time, transmission ranges and contention window sizes can be computed as the input to the performance model. Finally, values of transmission delay and throughput for each node are obtained as outputs from the network model. With the performance results and the density profile from the network model and the stochastic traffic model respectively, optimization for every location can be carried out. In the optimization block, PHY optimization determines the optimal value of the transmission range at every location and different time on the PHY layer of the 802.11p protocol. MAC optimization is used to find the optimal value of contention window size at homologous locations and time on the MAC layer. With the integration of both PHY and MAC optimization, the cross-layer optimization is gained and the final optimal values of the transmission range R_{op} and contention window size w_{op} for the cross layers are the outcomes of the optimization. In summary, given the velocity profile input, the outputs including the network performance results (delay and throughput) and the optimized performance with optimal values of transmission ranges and contention window sizes are obtained through our analytical modeling and optimization schemes.

The major contributions of this thesis are as follows:

1. Establishment of a two dimensional (2-D) Markov chain based contention model for characterizing the 802.11p channel access contention process of unicast in both the busy channel state and the idle channel state. For each node at different locations, the re-transmission mechanism and the exponential back-off procedure are considered once collisions happen under the stochastic traffic scenario.
2. Development of the interference model based on the foundation of the stochastic traffic model with the assumption of the Poisson arrival distribution, which analyzes packet collisions in the network. For the transmissions of nodes located at disparate positions, it may result in either simultaneous transmissions or hidden node collisions with overlapped transmission time between the senders and hidden nodes beyond the sensing range of those senders.
3. Development of the performance model considering the expected time slot between a busy channel time slot and an idle channel time slot to compose the failed transmission duration and the successful transmission duration for computing the delay and throughput of each node at every location.
4. Investigation of the effect induced from the realistic traffic distribution on the network performance through coupling the vehicular network with the signaling-lights-controlled urban traffic. This can be exploited for network performance prediction at each location as the substratum of preemptive traffic planning, road side units' deployment, traffic control and network planning (e.g. parameters optimization) for promoting the network efficiency.
5. Proposal of optimization methodologies for identifying the optimal parameter values (the optimal transmission range and the optimal contention window size)

based on the afore-hand VANET model estimation at different locations of the road. This information can be advertised to vehicles before joining the traffic stream for improving network performance while eliminating the measurement latency and cost triggered by observation and gauging work. The optimization encompasses PHY-layer optimization (deciding the optimal transmission ranges of nodes with the smallest sensing ranges for mitigating interference, meanwhile avoiding disconnection), MAC-layer optimization (finding the optimal contention window size to minimize collisions), and cross-layer optimization (implementing MAC optimization on the basis of PHY optimization).

6. Validation of 802.11p VANET unicast modeling by analytical performance results and simulated performance results acquired from the object-oriented simulation framework. The self-developed framework emulates the Poisson stochastic traffic and communications in the network with the consideration of the MAC layer channel access contention process and the interference condition.
7. Validation of the optimization methodologies by numerical results from the foresaid simulation framework with optimal values setup. Our results indicate that optimization results have prominent improvement compared with the original performance, specifically, MAC optimization generally possesses more increment than PHY optimization, and cross-layer optimization attains the highest performance.

1.2 Related Works

Most of the previous works in VANET performance analysis only depicted a homogeneous scenario for road traffic. For example, Ma et al. [4] put forward a one-dimensional (1-D) highway traffic model in which mobile vehicles were randomly distributed on the road according to the Poisson process. Nonetheless, this kind of models was unrealistic indeed. For the sake of describing more realistic traffic, the heterogeneous traffic flow was considered in [9]. A deterministic fluid dynamic model was applied for the heterogeneous traffic modeling and assessment of the density dynamics. The deterministic fluid dynamic model portrayed the fluid-like actions of moving vehicles on the traffic lane, and embodied the traffic flow adhering to the conservation law. [9] incorporated the situation of road intersections in traffic, and the number density of cars in jamming regions was also evaluated. There was plenty of boost on reality of traffic modeling in [9] by comparison with [4], even so, the traffic model in [9] was still not enough to be deemed as a realistic one. Since it could not characterize the randomness of individual vehicles, and it lacked considering the impact of traffic signaling lights and mutual effect of vehicles with both the intense jamming density pulse before the traffic light and the zero-density zone after the traffic light. Ho et al. [3] proposed a more reasonable stochastic traffic model for analyzing the vehicular traffic distribution to obtain a mean vehicular density profile as a function of space and time. The stochastic traffic model not only included the foregoing deterministic fluid dynamic model describing the mean behavior of the traffic stream, but also involved a stochastic model which delineated the random behaviors of individual vehicles without loss of generality. Moreover, the model approximated interaction of vehicles with the effect of traffic lights on the road. Through the model, road scenarios prediction can be realized so that vehicles traffic management and planning such as road system design, route formulation, congestion control and traffic signal configuration can then be carried out for increasing the traffic efficiency. As such, the stochastic traffic model in [3] is introduced for identifying the vehicle's traffic distribution in this thesis.

With respect to the modeling of the 802.11p MAC-layer contention process to access the channel, there is a re-transmission procedure for unicast, the 2-D Markov chain was commonly utilized in many previous studies. Bianchi et al. [10] proposed a 2-D Markov chain to acquire a relation between the transmission probability and probability of the collision brought by more than one concurrent transmitting nodes and/or hidden nodes for analyzing the performance of 802.11 protocol. Han [11] also established a 2-D Markov chain to analyze the throughput of the EDCA mechanism in 802.11p VANET, which improved the Markov chain in [10] by adding a re-transmission limit. Whereas, the alike shortcoming of both [10] and [11] was that no channel status (busy or idle) probability was considered in the sensing process of a node in the Markov chain. Wang et al. [12] designed a 2-D Markov chain, which took the channel condition probability in the sensing period into account for the augmentation of the multi-channel MAC protocol in IEEE

1609.4. It dwells on the multi-channel operation which enhances the functions of the MAC layer in 802.11p [13]. However, all of the above work did not bind vehicular networks with the practical traffic distribution in their contention modeling by the Markov chain. Qiu et al. [1] associated 802.11p network under the saturation scenario with the practical stochastic traffic model in [3] to represent a contention model based on a 1-D Markov chain for evaluating the broadcasting efficiency (ratio of vehicle's number with successful reception to the total vehicular number in the transmission region of a sender) for safety messages. In this thesis, the 2-D unicast Markov chain based contention model with sensing channel state probability and a retransmission limit by coalition of realistic traffic and 802.11p vehicular network is propounded.

In terms of VANET performance modeling, the important metrics delay and throughput are investigated. Bianchi [10] reckoned the delay as a set of expected time slots of which each one was the mean value of a successful packet transmission period, a failed packet transmission period and an idle period. The expected time slots modeling for delay was an ingenious approach. However, [10] just primitively treated a number of nodes as a whole network system, excluding a traffic distribution of nodes with the restricted transmission and interference range as only 802.11 network was studied. Likewise, the work of [1] was extended by [6] to model delay and throughput relying on the expectant of a transmission duration and an idle duration. [6] integrated both the practical traffic and the network to obtain the broadcasting delay and throughput of a node at a certain location. It further established the approximately average contention time for accessing channel in light of the expected time slots method and the Markov chain of the contention model, while the transmission time was not resolved in success and failure in this case as it was needless to guarantee transmission success for broadcasting. Consequently, both [10] and [6] were one-sided for unicast capability. This thesis synthesizes the expected time slot method, successful and failed transmission periods which are obtained from the stochastic traffic model and the contention model for the unicast performance estimation of each node at different locations in the VANET.

In relation to PHY-layer optimization, transmission power control for tuning the transmission range was commonly studied to minimize delay and shun collisions in the past. From [14], there were two distinct scenarios for transmitting power control in a network. They are respectively local transmission power control that every node altered its own power level and global transmission power control that all nodes were set to the identical transmitting power level. Local transmission power control was proved to be more effective for PHY-layer optimization in [14], and it was enabled by measurement of neighboring nodes' number and network performance parameters in many previous works. This could be implemented through the feedback-loop principle in [15] or local neighbor discovery in [16]. Guan [15] devised an algorithm in which the transmission power of each sender was rectified based on the number of nodes in vicinity beyond the required transmission range. The number of vicinal nodes was counted by feedback beacons' transmission from receivers. If the counter value of the number of nodes was larger than the predefined threshold *N*, it implies that there were superabundant nodes located beyond the demanded range and diminution of transmission power by a predefined delta value was supposed to be done. As the power regulation hinged on the feedback beacons' transmission on the channel, the channel fading condition was a key factor affecting the feedback loop. The fast-fading channel would damage some transmissions of feedback beacons. Therefore, the transmission power control scheme using feedback-loop principle in [15] was only adaptive for slow-fading channel. Whereas, channel fading would not be a problem for the local neighbor discovery method without feedback beacons' transmission. Tian et al. [16] raised a method named Connectivity Based Adaptive Transmit Power Control (C-ATPC) based on discovering the number of neighbors that vehicles transmitted the safety packet to one of their nearest neighbors, and next, those receivers added the sender vehicles' information to their own neighbor list. Then transmit power of each vehicle satisfying the required connectivity could be confirmed according to the vehicular number in the neighbor list. However, the weakness of local neighbor discovery was that nodes could not successfully receive all the safety packets due to interference during the neighbor discovery phase, so those nodes failed to know the exact number of adjacent nodes could not tune the transmit power well. Measuring the network performance parameter Packets Reception Rate (PRR), which was the proportion of the successfully received packets' number to the total number of packets sent, could overcome the weakness of local neighbor discovery. In [7], the transmission range of each vehicle was adapted by evaluating its PRR. Firstly, there was a sensing period for PRR measurement to compute the maximum achievable PRR. Afterwards, range adaption could be initiated that the transmission range ought to be lessened if the PRR threshold (minimum acceptable PRR) was larger than achieved PRR; or should be enlarged in the circumstance of the PRR threshold was lower than the achieved PRR; or stayed the same owing to the equivalence of the achieved value and the threshold of PRR. Nevertheless, all of the works in [7, 15-16] had a flaw that they engender delay and consume measurement overheads. This thesis presents a local transmission range adjustment scheme, which is based on the predictable vehicular density from the stochastic traffic model without measuring any data for each vehicle at different locations. Hence, there will be no more measurement delay and expense. Channel fading and the weakness of local neighbor discovery can absolutely be avoided for PHY-layer optimization either.

As for the MAC-layer optimization, classification of a service into different priority levels with different parameters was used in many previous works. Ma [17] conceived a scheme which classified the safety service into three levels with correspondingly distinctive contention window sizes to eliminate inter-level countdown collisions for mending the broadcast reliability. Level-one messages were highest-priority emergency warning messages with zero window size. Non-zero window size was assigned to the remaining two levels. In this way, dissemination reliability of emergent messages could be insured. In [18], the safety service broadcasted was also sorted into several priority levels with different Arbitration Inter-Frame Space Number values to ensure higher success rate for prioritized packets. However, the schemes in [17] and [18] were not suitable for unicast, because the ACK procedure had been present in unicast for securing reliability, and classification of a service would not make the unicast more reliable but only increase the complexity of channel access contention, especially considering that there had been already four types of services in 802.11p. In addition, coordination for deciding the sequence of nodes' transmissions could also optimize the performance. In [19], the Self-organizing Time Division Multiple Access (STDMA) was proposed for coordinating safety data transmission slots for broadcasting between vehicles, which outperforms traditional CSMA based ad-hoc vehicular networks. In essence, collisions were avoided through self-organizing of transmission slots at vehicular nodes in non-overlapping time frames. Qiu [20] estimated the throughput of a fully-coordinated broadcast scheme which resembled the STDMA in [19], and distinct positions in the channel access queue were assigned to every vehicle. However, coordination based methods are not appropriate for non-safety data unicast, in which long multimedia streams were usually transmitted. If the transmission time was coordinated, one node could wait for a long time before it could transmit, so instant messaging would not be able to be achieved. Moreover, there were some optimization methods which adjusted parameters by measuring the network load. Shen [21] developed a congestion control approach by adapting contention window size based on the measured channel load congestion for settling the collision problem to improve the network throughput. At first, a vehicle periodically measured the congestion condition, and the ratio of the number of queuing packets and unsuccessfully transmitted packets to the total number of packets was generated. Next, the vehicle doubled the contention window size till the preset maximum value to reduce collisions if the congestion condition was larger than the pre-established congestion threshold. Otherwise, the contention window size is halved till the initial value to shorten superfluous contention time. Analogously, Hsu [22] designed the Adaptive Offset Slot (AOS) mechanism to find the optimal contention window size by measuring the number of neighboring vehicles. The disadvantage of the works in both [21] and [22] was that there would be supererogatory delay caused by measuring procedures. Besides, another optimization method that searched optimal parameters for a data class within a confined space of allowable values (e.g. a certain number of contention window sizes from 4 to 256) was wielded by [23]. However, this method had low efficiency if there were vast permissible values in the search space. Finally, the derivative method, which was fitted for unicast with no measurement delay and low efficiency problem, was presented in many works. Rossi et al. [24] proposed an optimization approach that adapted the value of transmission probability following the dynamics of vehicles' density to maximize the throughput by the mathematical derivative deduction method. In the optimization approach, the throughput of a node to its adjacent node was analyzed to be expressed as a function of transmission probability, vehicular density and other network parameters. After that, the first derivative of throughput with reference to the transmission probability was found, and the optimal transmission probability could be determined by imposing the derivative equal to zero. Patras [25] and Bianchi [10] exerted adaptive techniques on tuning contention window size to achieve respectively the optimal collision probability and the optimal transmission rate through the derivative of the throughput. Wang [26] directly computed the derivative of the saturation throughput and a function of contention window size w to accrue the optimal value of w depending on the number of vehicles. Nonetheless, among all the optimization approaches mentioned above, some of them lost the sight of vehicular traffic. In some others, only homogeneous traffic with Poisson arrival or highway traffic was considered for network modeling, the former traffic was not in line with the practical traffic scenario in urban area. In light of these inadequacies, a MAC-layer optimization method combining the derivative with an efficient iterative search method is proposed in this thesis, which identifies the optimal contention window size for each vehicle at different locations under the stochastic traffic model and network model in Section 1.1.

In sum, this thesis models the unicast performance of 802.11p VANETs and optimizes the delay and throughput performance. Part of the contents in this thesis have been published in [27].

1.3 Organization of the Thesis

The remainder of this thesis is structured as follows. Chapter 2 briefly introduces the vehicular ad-hoc network with 802.11p protocol. In chapter 3, the stochastic traffic model is stated to reflect the realistic traffic scenario. We model the 802.11p unicast contention process of vehicles to access the channel by a two-dimensional Markov chain in chapter 4. Chapter 5 proposes an interference model for analyzing collisions for data transmissions. In chapter 6, network performance including delay and throughput is estimated. In chapter 7, optimization methods for PHY layer, MAC layer and cross layer are specified. Chapter 8 concisely describes the simulation framework and gives numerical results with correlated discussions. Validation of analytical model accuracy and optimization are achieved. Chapter 9 summarizes the thesis and outlines possible directions for future work.

Chapter 2 The VANETs and IEEE 802.11p Protocol

In this chapter, the overview of VANET is concisely stated in section 2.1. The introduction of two categories of data (safety data and non-safety data) to be transmitted in VANETs are also included in that section. Section 2.2 firstly narrates the bandwidth allocation for the 802.11p channels, and subsequently lists the EDCA parameters. At last, the 802.11p medium access process is specified.

2.1 The Overview of VANETs

The Vehicular Ad-Hoc Network (VANET) is the mobile network formed by moving vehicles as network nodes with Road Side Units (RSU) or infrastructures for ubiquitous wireless access. It focuses on inter-vehicle and vehicles-to-infrastructures connections. The overview scenario of VANETs is displayed in Figure 2.1 [28]. The VANETs can stand alone, or can be concatenated to Internet via base stations or network access points.

VANETs can furnish pervasive transmission services for safety data (vehicles' velocity and location, warning information such as turning, braking, acceleration, overtaking, etc.), as well as non-safety data including infotainment information, sensor data (object movements, lane tracking, etc.) and 3D laser data (contours of environment and shapes of objects). The safety data is usually regarded as the "heartbeat" or "beacon packet" with a constant packet size. As an illustration, the broadcast of safety messages in 802.11p VANETs was studied in [1]. Furthermore, advertisement (as infotainment) dissemination can be addressed in the non-safety data transmission for promoting commercial profits. In [29], a shadow-toll-based model supported with digital advertising superimposed on physical billboards was raised to attract investment from advertisers for benefits increment in addition to traditional toll station revenues. The model was implemented by employing communications between vehicles and roadside infrastructures.

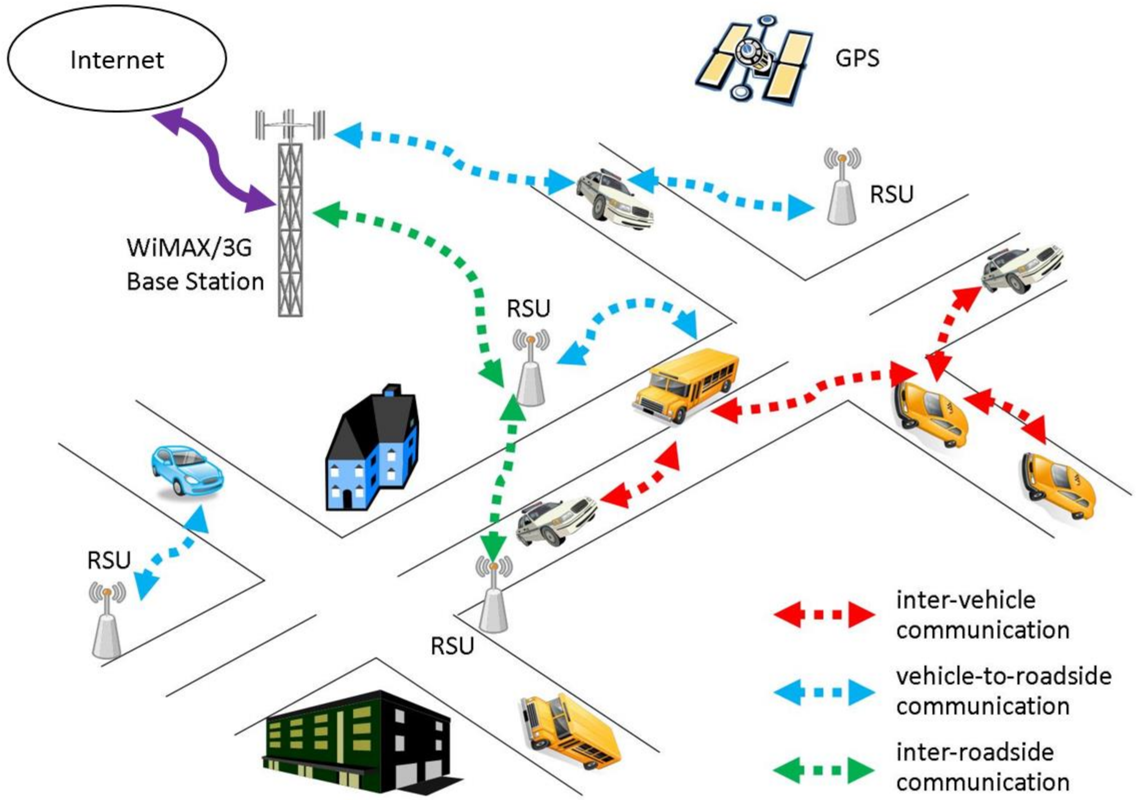

Figure 2.1. The overview scenario of VANETs [28].

2.2 Introduction of 802.11p

IEEE 802.11p defines the physical and MAC layers in the Dedicated Short Range Communications (DSRC) protocol stack for communications in VANETs. From [5], the 802.11p is an amendment to the IEEE 802.11 standard used in the Wireless Local Area Network (WLAN), which inherits Physical-layer protocols from 802.11a Orthogonal Frequency Division Multiplexing (OFDM) and the Enhanced Distribution Channel Access (EDCA) Media Access Control mechanism from 802.11e [30] with differentiation on services priorities.

2.2.1 802.11p Channels

The DSRC band with the licensed bandwidth 75 MHz from 5.85 GHz to 5.925 GHz is allocated for vehicular communication [31-32]. In DSRC, the band is divided into seven channels with 10 MHz for each one. One of the seven channels is used as the control channel (CCH) for the safety messages transmission, and the others are used as service channels (SCH) for the non-safety information transmission. The rest 5 MHz is used as the guard bandwidth. Figure 2.2 [32] shows the frequency allocation of channels for Wireless Access in Vehicular Environments (WAVE). In 802.11p, the CCH and the SCH switch with each other every 50 ms according to the IEEE 1609.4 standard [13].

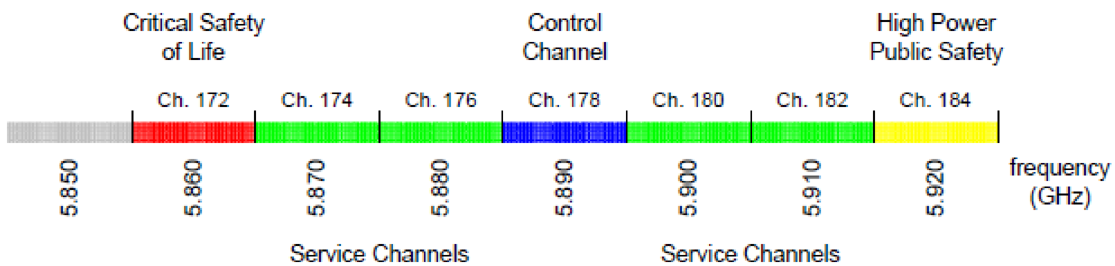

Figure 2.2. 802.11p WAVE channels [32].

2.2.2 802.11p EDCA Parameters and the Medium Access Procedure

There are four access classes (AC) of data prioritized from Access Class 3 (AC 3) to Access Class (AC 0) with different values of the Contention Window size (*CW*) and the Arbitration Inter-Frame Space (AIFS), as shown in Table 2.1 [1] as follows. AIFS is the idle channel time interval that a node should wait before the back-off procedure in which the node subtracts one from a random integer in [0, *CW*] for each elapsing idle time slot until the integer (or counter value) reaches zero. When the counter reaches zero, the node starts transmitting. Naturally, *CW* is the maximum value that the random integer can possibly be. Values of *CW* and AIFS in the table signify the number of time slots for the count down. Defined in 802.11p, a time slot is equal to 16 μs. The smaller the values of *CW* and AIFS indicate the higher priority for the data class, so AC 3 possesses the highest priority. Every node maintains four buffers for four discriminative data class queues.

Table 2.1. EDCA parameters in IEEE 802.11p [1].

AC	Data Class	CW_{min}	CW_{max}	AIFS
3	Video/ Safety related	3	7	2
2	Voice	3	7	3
1	Best Effort	7	15	6
0	Background Traffic	15	1023	9

Figure. 2.3 depicts the basic scenario of the 802.11p medium access procedure for all the four ACs in accordance with EDCA parameters in Table 2.1. 802.11p uses the Carrier Sense Multiple Access with Collision Avoidance (CSMA/CA) [1, 11] medium access mechanism.

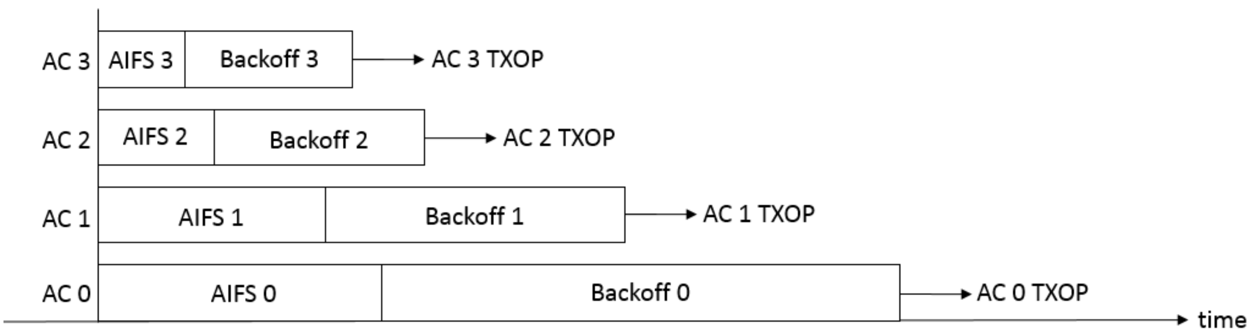

Figure 2.3. The basic medium access procedure in 802.11p.

With Table 2.1 and Figure 2.3 above, the CSMA/CA medium access procedure with four essentials is listed in the following.

1) Each AC in every node maintains a contention counter assigned with a random integer sliding between 0 and CW_{min}: [0, CW_{min}].
2) During the busy interval of the channel sensed by a node, the contention counter of the AC in the node keeps frozen. But after the channel sensed is idle for the duration of AIFS, back-off countdown of the contention counter is initiated, it decreases by one for each passing idle slot. If the channel sensed is busy in the process of countdown, the contention counter will be suspended, and will then restart countdown directly from the suspended contention value without waiting another AIFS once the channel is idle again. When the contention counter reaches zero, the first packet in the AC queue is transmitted on the channel. After each successful transmission, CW will be reset to CW_{min}.
3) The collision is defined that if there exists at least one concurrent time slot during

which two or more nodes including the hidden nodes within the sensing range of a vehicle transmit and the vehicle is the receiver of one or more transmitting nodes, the messages sent to the vehicle as the receiver from the sender will be corrupted. The collision is also called the external collision and causes the transmission failure. Then the exponential back-off process in the sender starts: the packet is retransmitted with the doubled contention window size, and then the contention counter will be set with a random integer newly picked from [0, $2CW_{min}$ - 1]; after the channel is idle for a duration of AIFS, countdown repeats; if the retransmission upon collisions remains occurring, the contention window size will be accumulatively doubled until the stipulated maximum value CW_{max}; in some cases, with a certain number of retransmission times after CW_{max} is reached, the retransmission of the packet will not continue as the packet will be obsoleted, and CW will be scheduled back to CW_{min}.

4) If more than one AC queue in a node initiate coinstantaneous transmissions, which is called the internal collision, the scheduler inside the node will grant the transmission opportunity (TXOP) to the highest-priority transmitting AC queue. But for the rest of collided AC queues, the exponential back-off procedure will be kicked off.

Chapter 3 The Stochastic Traffic Model

This chapter is a summary of the work in [3] which provides a succinct description of a realistic traffic model, the stochastic traffic model, for urban road systems, as well as the interoperable effect among vehicles of which movement is harnessed by signalized traffic lights. Section 3.1 gives an overview of the traffic model, including the one-dimensional road scenario in urban area and the generalization of the process from the input (velocity profile) to the output (mean vehicular density) through modeling. There are two compositions of the stochastic traffic model. One is the deterministic fluid dynamic model which specifies the vehicular density dynamics and will be presented in Section 3.2. Section 3.3 introduces the stochastic model which is the other composition delineating the randomness of vehicular traffic with the probability distribution. Finally, the approximation of vehicular interactions is presented in Section 3.4.

3.1 The Overview of the Model

This thesis considers urban traffic. In urban area, the giant city-wide traffic roads layout between diverse constructions is composed of many roads crossing each other along with traffic lights deployed for traffic control. The urban traffic can be split into numerous one-dimensional (1-D) roads which sketch a one-directional, single-lane and semi-infinite scenario as depicted in Figure 3.1. The 1-D road is divided into many segments with traffic lights located at the junctions of any two adjacent road segments. The location space of the road is delimited in the semi-infinite region $[0, \infty)$, and vehicles arrive at location 0 as the start point, move toward the right direction. Vehicles can join or leave the road at junctions downward. More complicated road topology including multiple-directional, multiple-lane, and curved roads can be superposed by a set of different 1-D road segments.

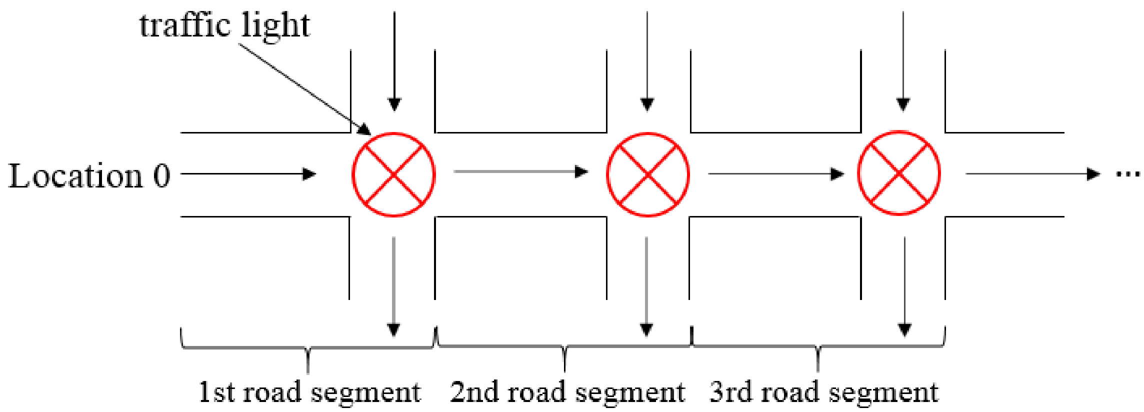

Figure 3.1. The 1-D road scenario.

A stochastic traffic model from [3] based on the 1-D road system above is proposed to lay the foundation for the network modeling of vehicular communications. The stochastic traffic model embraces two components, namely the deterministic fluid dynamic model and the stochastic model. The deterministic fluid dynamic model characterizes the evolving progress of the traffic flow and deduces a fundamental ordinary differential equation (ODE) so as to compute the density of vehicles, while the stochastic model presents the random fluctuations of the number of vehicles for estimation of the probability distribution. Besides, the presence of the traffic light effect on the distribution of vehicles is modeled through a density-dependent vehicular velocity profile, which serves as the input to the stochastic traffic model. Finally, interactions among vehicles can be approximated. With the velocity profile input and additional signaling information (traffic lights' locations, red light period, mean free speed setting, etc.), the analytical mean vehicular density profile as the output of the stochastic traffic model can be derived by the solution of the ODE. The stochastic traffic model with approximation of vehicles interactions have been evaluated by simulations and corroborated with real-world empirical data in [3].

3.2 The Deterministic Fluid Dynamic Model

The deterministic fluid dynamic model is a kind of continuum traffic flow model which demonstrates the spatial and temporal dynamics of mobility trace. We model the traffic flow on the road from location 0 to any location x to derive the fluid conservation equation and subsequently identify the ODE for the computation of vehicular density.

The traffic flow on the road region [0, x] in Figure 3.1 can be represented in Figure 3.2. Vehicles arrive at location 0 with the arrival process $\{A(t) \mid -\infty < t < +\infty\}$ which describes the number of arrivals to the 1st road segment up to time t. Then the non-negative and integrable arrival rate (arrival number of cars in one time unit) can be expressed as $\alpha(t) = dA(t)/dt$, $\alpha(t) \geq 0$. $C^+(x, t)$ denotes the aggregated number of vehicles which enter the road by arriving at location 0 and joining through all the junctions configured within the space range (0, x] during the time interval ($-\infty$, t], and $C^-(x, t)$ correspondingly represents the total number of vehicles leaving from location (0, x] through junctions before time t. $Q(x, t)$ signifies the number of vehicles moving past location x until time t. Then the subsistent number of vehicles within the region (0, x] at time t can be stated as $N(x, t)$.

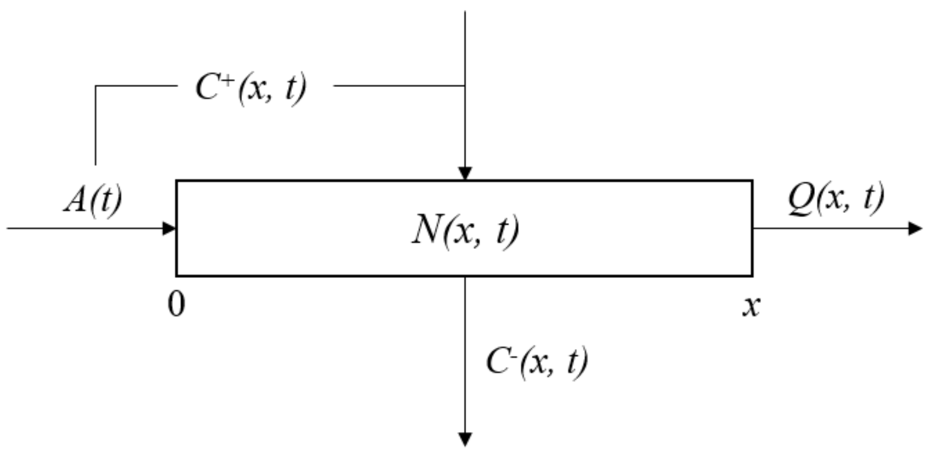

Figure 3.2. Traffic flow.

Thus, the fluid conservation equation can be obtained as

$$N(x,t) = C^+(x,t) - C^-(x,t) - Q(x,t). \tag{1}$$

With four parameters $N(x, t)$, $C^+(x, t)$, $C^-(x, t)$ and $Q(x, t)$, relevant density functions and flow rate function can be derived. At location x and time t, the vehicular density can be expressed as

$$n(x,t) = \frac{\partial N(x,t)}{\partial x}. \tag{2}$$

The entering rate density can be

$$c^+(x,t) = \frac{\partial^2 C^+(x,t)}{\partial x \partial t}. \quad (3)$$

while the leaving rate density is

$$c^-(x,t) = \frac{\partial^2 C^-(x,t)}{\partial x \partial t}. \quad (4)$$

The flow rate is defined as

$$q(x,t) = \frac{\partial Q(x,t)}{\partial t}. \quad (5)$$

By implementing $\partial^2/\partial t \partial x$ operation on (1) with substitution of (2), (3), (4) and (5), a partial differential equation (PDE) is acquired below,

$$\frac{\partial n(x,t)}{\partial t} = c^+(x,t) - c^-(x,t) - \frac{\partial q(x,t)}{\partial x}. \quad (6)$$

Let $v(x,\ t)$ be the velocity of a vehicle as a function of location x and time t. With the fundamental relation $q(x, t) = n(x, t)v(x, t)$ (flow = density * velocity) in light of the traffic flow theory, (6) can be transformed to

$$\frac{\partial n(x,t)}{\partial t} = c^+(x,t) - c^-(x,t) - \frac{\partial [n(x,t)v(x,t)]}{\partial x}. \quad (7)$$

The mean behavior of the stochastic traffic model is governed by the PDE in (7). For convenience of solving (7), the PDE could be converted to an ODE. Let $x(t)$ be the location function varying by time t, then

$$\frac{\mathrm{d}x(t)}{\mathrm{d}t} = v(x(t),t). \quad (8)$$

Applying the chain rule, we have

$$\frac{\mathrm{d}n(x(t),t)}{\mathrm{d}t} = \frac{\partial n(x,t)}{\partial x}\frac{dx(t)}{dt} + \frac{\partial n(x,t)}{\partial t}. \quad (9)$$

By substituting (7) and (8) into (9), if $v(x, t)$ is independent of $n(x, t)$, the ODE for valuation of vehicular density profile can be found as follows,

$$\frac{dn(x,t)}{dt} = c^+(x,t) - c^-(x,t) - \frac{\partial v(x,t)}{\partial x} n(x,t). \quad (10)$$

With the knowledge of the entering rate density $c^+(x, t)$, leaving rate density $c^-(x, t)$ and the velocity profile $v(x, t)$, (10) can be solved to obtain the vehicular density $n(x, t)$. In this thesis, it is assumed that vehicles enter the road only by arriving at the first road segment at a rate $\alpha(t)$ without joining at junctions, and there are no vehicles leaving from junctions either. Hence, $c^+(x, t) = \alpha(t)\delta(x)$ and $c^-(x, t) = 0$, where $\lim_{\varepsilon \to 0} \int_{x-\varepsilon}^{x+\varepsilon} \delta(y)\, dy = 1$ if $x = 0$, and 0 otherwise. The velocity profile $v(x, t)$ is given in Section 3.4 later on.

3.3 The Stochastic Model

The fluid model per se is incapable of capturing the variability of vehicles' random behaviors. In order to supplement this shortage, the stochastic model as the probabilistic form of the fluid model is proposed to obtain the probability distribution of randomness. In the stochastic realm, from time $t = 0$, there are many possible scenarios about the density and number of vehicles at different time. Thus all the deterministic variables $N(x, t)$, $C^+(x, t)$, $C^-(x, t)$ and $Q(x, t)$ in the fluid model are now probabilistic variables. Henceforth, $n(x, t)$, $c^+(x, t)$, $c^-(x, t)$ and $q(x, t)$ are used to denote the average probability density function (PDF) or rate by the differential of the expected values of the four probabilistic variables foresaid as

$$n(x,t) = \frac{\partial E[N(x,t)]}{\partial x}, \tag{11}$$

$$c^+(x,t) = \frac{\partial^2 E[C^+(x,t)]}{\partial x \partial t}, \tag{12}$$

$$c^-(x,t) = \frac{\partial^2 E[C^-(x,t)]}{\partial x \partial t}, \tag{13}$$

and

$$q(x,t) = \frac{\partial E[Q(x,t)]}{\partial t}. \tag{14}$$

Then the PDE in (6) and ODE in (10) are of mean forms, so that the mean vehicular density as the average PDF can be found by solving the mean ODE.

If the velocity profile $v(x, t)$ is not a function of the car density $n(x, t)$ and the arrival process $\{A(t) \mid -\infty < t < +\infty\}$ with the average arrival rate $\alpha(t)$ obeys Poisson process, two properties hold in the following.

Property 1: The expected values of the random variables $N(x, t)$ and $Q(x, t)$ following the Poisson distribution can be computed through

$$E[N(x,t)] = \int_{\sigma(x,t)}^{t} \alpha(s) ds \tag{15}$$

and

$$E[Q(x,t)] = \int_{-\infty}^{\sigma(x,t)} \alpha(s)ds, \tag{16}$$

where $\sigma(x, t)$ indicates the road entrance time of a vehicle that remains in the road region $(0, x]$ at time t. We define that vehicles arriving to the road before $\sigma(x, t)$ have passed location x by time t, while vehicles arriving after $\sigma(x, t)$ must still be in the region $(0, x]$ at time t as the road considered is one-directional and single-lane so that overtaking impossibly arises.

Property 2: The numbers of vehicles in two non-overlapping regions $(x_1, x_2]$ and $(x_3, x_4]$ at time t are independent and can be expressed with means

$$\overline{N}(x_1, x_2, t) = E[N(x_1, x_2, t)] = \int_{x_1}^{x_2} n(x,t)dx, \tag{17}$$

$$\overline{N}(x_3, x_4, t) = E[N(x_3, x_4, t)] = \int_{x_3}^{x_4} n(x,t)dx, \tag{18}$$

3.4 Vehicles Interactions

Interactions between vehicles can be approximated to attain the vehicular density profile with the velocity profile as the input. The existence of traffic signaling lights in urban area, which halt vehicles during the red signal period, should be taken into consideration. Thus, the compression of vehicles before the traffic light and the release of vehicles after the traffic light are modeled by shockwave and a density-dependent velocity profile can be reaped as follows,

$$v(x,t) = v_f\left(1 - \frac{n(x,t)}{k_j}\right), \tag{19}$$

where v_f is the mean free speed, and k_j is the jamming density (congested number of cars that occupy in a space unit). From (19), velocity will become lower or higher when density ascends or descends. The velocity is set to zero at the crossing zone during the red light interval.

In order to capture the propagation of shockwave, the front-density-dependent velocity based on (19) is proposed as

$$v(x,t) = v_f\left(1 - \frac{n(x+\Delta x, t)}{k_j}\right). \tag{20}$$

The velocity in (20) is a function of density with Δx in front of location x as the displacement of a function of density at certain location x in (19). It means that when the vehicular density in front goes up on account that preceding cars retard or stop, the vehicles at location x will decelerate or pause moving correspondingly. On the other hand, if the vehicles in front accelerate so that the density decreases, the following cars will accelerate accordingly.

Therefore, the approximation of vehicular interactions can be done by initializing the vehicular density to 0 for all x along the road (i.e., $n(x, 0) = 0$), iteratively obtaining the front-density-dependent velocity profile $v(x, t)$ from vehicular density according to (20) as the input to the stochastic traffic model, and iteratively solving the ODE (10) in the deterministic fluid dynamic model with the input velocity and signaling information (such as locations of traffic lights, red traffic light period and mean free speed configuration) at different locations until the pre-defined end time of the system. Finally the vehicular density profile is generated as the output of the whole stochastic traffic model.

What should be noticed is that, with the introduction of the front-density-dependent velocity profile (20), the equation (10) is no longer an ODE and the two properties in the stochastic model will be invalid. Even so, we still solve the ODE (10) and use the stochastic model as an approximation in this thesis, since there is only an inconspicuous impact of density $n(x, t)$ on velocity $v(x, t)$ given that the arrival rate is less than 30 cars/min according to the result in [3]. We can easily gather the empirical mobility traces to verify the accuracy of the 1-D stochastic traffic model. For further details regarding the stochastic traffic model, the reader is referred to [3].

Chapter 4 The Contention Model of 802.11p Unicast

In this chapter, the access contention mechanism of 802.11p unicast is modeled by a 2-D Markov chain based on the vehicular density profile derived from the stochastic traffic model foresaid in the previous chapter. Section 4.1 gives an overview of the model, lists assumptions on both the PHY layer and the MAC layer, and finally epitomizes the modeling methodology. In Section 4.2, the 2-D Markov chain is presented and the stationary distribution of the Markov chain is mathematically solved to find the expression for the transmission probability.

4.1 The Model Overview

Hereon, we model the contention process of channel access for non-safety message unicast transmissions in V2V communications of 802.11p VANETs. There are four data classes for non-safety messages with four channel access priorities respectively as illustrated Table 2.1. In this thesis, we only focus on the packet transmission of the highest-priority access class. Thus, only the single access class queue in a node for the transmission is considered. In addition, six SCHs are used for the non-safety data transmission, and this thesis only investigates the single-channel transmission for simplification. Scenarios of multiple queues and/or multiple channels can be readily analyzed by extending our work.

For the ease of modeling the contention, some assumptions are made as follows.

Assumptions on the PHY layer:

1). The channel is isotropic and homogeneous along the road.
2). The transmission range and sensing range of a vehicle is denoted as R_S and R_I respectively, where $R_S < R_I$. The transmission range R_S of every vehicle is identical, and every vehicle also has the same sensing range R_I. Vehicles within the

transmission range R_S of a transmitter are able to receive packets successfully if there is no collision. Vehicles within the sensing range R_I of a transmitting node can sense the transmission, and are interfered by the transmitter. So the sensing range R_I is also regarded as the interference range.

3). Transmission failure in the system is uniquely caused by packet collision (of which the definition has been stated in chapter 2). Other possible causes such as the transmission error, the coding error, channel fading, etc. for the transmission failure are ignored. What is worthy of mention is that the link breaking that the receiver moves out of the transmission range of the sender in its transmission duration can also be neglected, because the velocity of mobile vehicles is relatively low compared with the data transmission rate and the vehicles can be deemed as static during the transmission of a packet.

Assumptions on the MAC layer:

1). In view of the multimedia stream information and application transmission by unicast, we only consider the saturated condition that there are continuous packets available for transmissions during the SCH interval to make a perpetual non-empty queue.

2). The channel time is regarded as infinitely long so that packet transmission will not be ceased due to channel switches [6].

3). All nodes share the same EDCA setting.

As the 2-D Markov chain is applicable for characterizing the retransmission procedure of unicast, like many previous works, this thesis also adopts the 2-D Markov chain for describing the contention process of 802.11p unicast. Whereas, many other works lacked considering the vehicular traffic in the 2-D Markov chain they used. This thesis bridges the realistic traffic model with vehicular networks by introducing the busy channel probability p, which is highly correlated to the vehicular traffic distribution, into the 2-D Markov chain. We build a contention model for generating the transmission probability of a car as a function of the collision probability for the packet transmitted from the car, given the vehicular density profile $n(x, t)$ as the input from the stochastic traffic model.

4.2 The Contention Model based on a 2-D Markov Chain

Given that there is a car at location a (or simply car a), the 2-D Markov chain is established as shown in Figure 4.1 to model the 802.11p unicast contention process of a single access class in the car according to the CSMA/CA medium access mechanism. It is for analyzing the probability τ for car a to transmit a packet at the beginning of a time slot. The AIFS is omitted for convenience of analysis, and it can be easily brought into the Markov chain by adding extra states. The definition of the notations used in the Markov chain is tabulated in Table 4.1. Note that every passing time slot in the Markov chain is actually the expected value of a busy time interval of T physical slots (as channel will be busy for a transmission duration of T slots for a packet every time) with probability p and an idle physical slot with probability 1 - p. A physical slot here is actually a time slot with 16 μs (declared in Chapter 2). The length of an expected time slot is equal to $pT + (1 - p)$ according to [6].

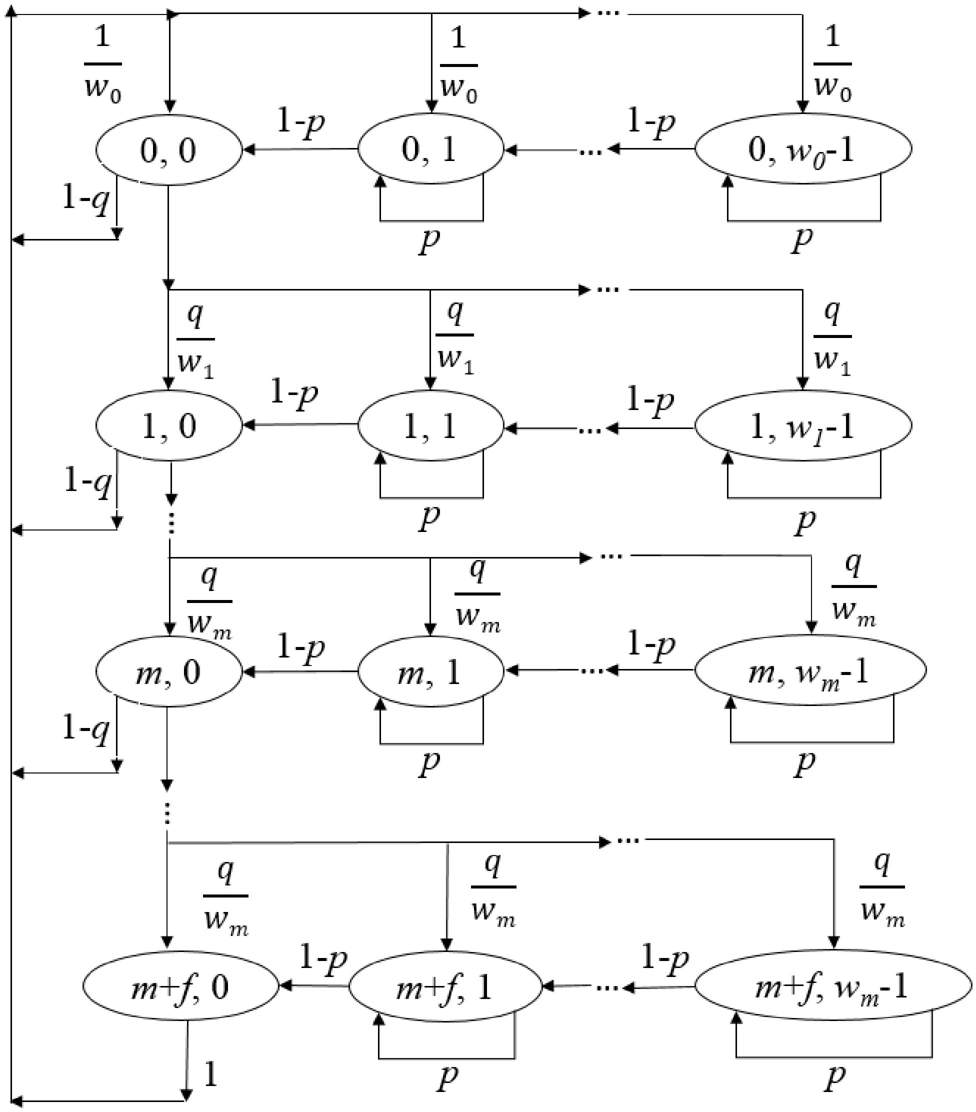

Figure 4.1. The 2-D Markov chain for a single access class in 802.11p unicast.

Table 4.1. Notations used in the 2-D Markov chain.

Notation	Definition
<i, k>	each state: i means the back-off stage (the number of collisions that one packet has suffered), and k is the back-off counter value
p	the probability that the channel sensed by the car at location a is busy
w_i	the total number of counter values for the contention window size at stage i, and $w_i = CW_i + 1$
q	collision probability of the packet transmitted from the car at location a
m	the maximum times for the initial contention window size to be doubled
f	the maximum number of retransmissions after stage m and before the packet is discarded

The channel sensed by the car at location a is busy if there is at least one car transmitting within car a's sensing range R_I. According to the empirical result in [3], we assume that the number of cars in the road is Poisson distributed. Then, we have the busy channel probability p expressed with the Taylor formula as

$$\begin{aligned} p &= 1 - \sum_{n=0}^{\infty} P(n \text{ cars in the sensing range}) \left(1 - \tau_{R_I}\right)^n \\ &= 1 - \sum_{n=0}^{\infty} \frac{\bar{N}_{R_I}{}^n e^{-\bar{N}_{R_I}}}{n!} \left(1 - \tau_{R_I}\right)^n \\ &= 1 - e^{-\bar{N}_{R_I} \tau_{R_I}}, \end{aligned} \tag{21}$$

where τ_{R_I} is the average transmission probability for all cars within car a's sensing range, and $\bar{N}_{R_I}$ is the mean number of cars in the sensing range of car a. Since a SCH interval of 50 ms is extremely small, the density profile $n(x, t)$ barely varies and the vehicular distribution can be seen as static during the SCH interval. Thus, we elide t in $n(x, t)$ for simplicity. From (17) and (18), we have $\bar{N}_{R_I} = \int_{a-R_I}^{a} n(x)dx + \int_{a}^{a+R_I} n(x)dx$.

In order to find the transmission probability expression as a function of collision probability, we solve the stationary distribution of the 2-D Markov chain in Figure 4.1. By denoting the maximum contention window size at stage i with w_i,

$$\begin{aligned} w_0 &= CW_{\min} + 1, \\ w_m &= CW_{\max} + 1. \end{aligned} \tag{22}$$

We also have

$$w_i = \begin{cases} 2^i w_0, & for\ 0 \le i \le m \\ 2^m w_0, & for\ m < i \le m+f \end{cases}. \tag{23}$$

According to the property of the Markov chain, system entering probability = system exiting probability. Let the probability in state <*i*, *k*> be $b_{i,k}$. If we regard states {[*i*, 0], [*i*, 1], [*i*, 2] … [*i*, w_i – 1]} as a system, the following expression can be obtained,

$$qb_{i-1,0} = b_{i,0},\ \ for\ 1 \le i \le m+f\ . \tag{24}$$

If we do some simple transformations on (24), we can derive

$$b_{i,0} = q^i b_{0,0}\ ,\ \ for\ 0 \le i \le m+f\ . \tag{25}$$

Next, if we focus on system {[*i*, 1], [*i*, 2] … [*i*, w_i - 1]}, system {[*i*, 2], [*i*, 3] … [*i*, w_i - 1]}, system {[*i*, 3], [*i*, 4] … [*i*, w_i - 1]} … system {[*i*, w_i - 1]} in turn, we can conclude that

$$(1-p)b_{i,k} = q\frac{w_i - k}{w_i} b_{i-1,0}\ ,\ \ for\ 1 \le i \le m, 1 \le k \le w_i - 1 \tag{26}$$

and

$$(1-p)b_{i,k} = q\frac{w_m - k}{w_m} b_{i-1,0}\ ,\ \ for\ m+1 \le i \le m+f, 1 \le k \le w_m - 1. \tag{27}$$

Treating states {[0, 1], [0, 2] … [0, w_0 - 1]} as a system and similarly considering states {[0, 2], [0, 3] … [0, w_0 - 1]} … {[0, w_0 - 1]} as different systems, we can get

$$(1-p)b_{i,k} = (1-q)\frac{w_0 - k}{w_0}\sum_{i=0}^{m+f-1} b_{i,0} + \frac{w_0 - k}{w_0} b_{m+f,0}\ ,\ \ for\ i = 0, 1 \le k \le w_0 - 1. \tag{28}$$

Substituting (25) into (28), we have

$$b_{i,k} = \frac{1}{1-p}\frac{w_0 - k}{w_0} b_{0,0}\ ,\ \ for\ i = 0, 1 \le k \le w_0 - 1. \tag{29}$$

By combining (24), (25), (26), (27) and (29), a set of expressions can be summarized below,

$$b_{i,k}=\begin{cases} q^i b_{0,0}\,, & for\ 0\le i\le m+f, k=0 \\ \dfrac{1}{1-p}\dfrac{w_i-k}{w_i}q^i b_{0,0}\,, & for\ 0\le i\le m, 1\le k\le w_i-1 \\ \dfrac{1}{1-p}\dfrac{w_m-k}{w_m}q^i b_{0,0}\,, & for\ m+1\le i\le m+f, 1\le k\le w_m-1 \end{cases} \quad . \tag{30}$$

In light of another property of the Markov chain, the summation of probability in all states equals to 1, $\sum P\_State = 1$. Therefore,

$$\begin{aligned} 1 &= \sum_{\mathrm{i}=0}^{m+f}\sum_{k=0}^{w_i-1} b_{i,k} \\ &= \sum_{i=0}^{m+f} b_{i,0} + \sum_{\mathrm{i}=0}^{m}\sum_{k=1}^{w_i-1} b_{i,k} + \sum_{\mathrm{i}=m+1}^{m+f}\sum_{k=1}^{w_m-1} b_{i,k} \end{aligned} \quad . \tag{31}$$

Let

$$A=\sum_{i=0}^{m+f} b_{i,0}\,, \tag{32}$$

$$B=\sum_{\mathrm{i}=0}^{m}\sum_{k=1}^{w_i-1} b_{i,k}\,, \tag{33}$$

and

$$C=\sum_{\mathrm{i}=m+1}^{m+f}\sum_{k=1}^{w_m-1} b_{i,k}\,. \tag{34}$$

According to (30) and (32),

$$\begin{aligned} A &= \sum_{i=0}^{m+f} b_{i,0} \\ &= \sum_{i=0}^{m+f} q^i b_{0,0} \\ &= b_{0,0}\frac{1-q^{m+f+1}}{1-q} \end{aligned} \quad . \tag{35}$$

From (23), (30) and (33), we can obtain

$$
\begin{aligned}
B &= \sum_{i=0}^{m}\sum_{k=1}^{w_i-1} b_{i,k} \\
&= \frac{1}{1-p} b_{0,0} \sum_{i=0}^{m} q^i [\sum_{k=1}^{w_i-1}(1-\frac{k}{w_i})] \\
&= \frac{1}{1-p} b_{0,0} \sum_{i=0}^{m} q^i \, \frac{w_i-1}{2} \\
&= \frac{1}{2(1-p)} b_{0,0} [w_0 \sum_{i=0}^{m}(2q)^i - \sum_{i=0}^{m} q^i] \\
&= b_{0,0} \frac{1}{2(1-p)} (w_0 \frac{1-(2q)^{m+1}}{1-2q} - \frac{1-q^{m+1}}{1-q})
\end{aligned}
\quad . \tag{36}
$$

By (30) and (34), the following expression is given,

$$
\begin{aligned}
C &= \sum_{i=m+1}^{m+f}\sum_{k=1}^{w_m-1} b_{i,k} \\
&= \frac{1}{1-p} b_{0,0} \sum_{i=m+1}^{m+f} q^i [\sum_{k=1}^{w_m-1}(1-\frac{k}{w_m})] \\
&= \frac{1}{2(1-p)} b_{0,0} \sum_{i=m+1}^{m+f} q^i (w_m-1) \\
&= b_{0,0} \frac{w_m-1}{2(1-p)} \frac{q^{m+1}(1-q^f)}{1-q}
\end{aligned}
\quad . \tag{37}
$$

Finally, we summarize from (31) to (37) that

$$
\begin{aligned}
1 &= A+B+C \\
&= b_{0,0}[\frac{1-q^{m+f+1}}{1-q} + \frac{1}{2(1-p)}(w_0 \frac{1-(2q)^{m+1}}{1-2q} - \frac{1-q^{m+1}}{1-q}) + \frac{w_m-1}{2(1-p)} \frac{q^{m+1}(1-q^f)}{1-q}]
\end{aligned}
\cdot \tag{38}
$$

Then

$$
b_{0,0} = [\frac{1-q^{m+f+1}}{1-q} + \frac{1}{2(1-p)}(w_0 \frac{1-(2q)^{m+1}}{1-2q} - \frac{1-q^{m+1}}{1-q}) + \frac{w_m-1}{2(1-p)} \frac{q^{m+1}(1-q^f)}{1-q}]^{-1} . \tag{39}
$$

At every back-off stage i in the Markov chain, the car will transmit when the back-off counter value k reaches zero. Then the overall transmission probability of the car can be mathematically expressed as the summation of probability in states <i, 0>. Thus, we have the following expression with substitution of (30),

$$\begin{aligned}\tau &= \sum_{i=0}^{m+f} b_{i,0} \\ &= \sum_{i=0}^{m+f} q^i b_{0,0} \\ &= \frac{1-q^{m+f+1}}{1-q} b_{0,0}\end{aligned} \quad . \tag{40}$$

Substituting (39) into (40), we have

$$\tau = \frac{1-q^{m+f+1}}{1-q}\left[\frac{1-q^{m+f+1}}{1-q} + \frac{1}{2(1-p)}\left(w_0 \frac{1-(2q)^{m+1}}{1-2q} - \frac{1-q^{m+1}}{1-q}\right) + \frac{w_m-1}{2(1-p)} \frac{q^{m+1}(1-q^f)}{1-q}\right]^{-1}. \tag{41}$$

The form of (41) varies as the parameters m and f are assigned with different values. If we set $m = 0$ and $f = 0$, i.e., there is no retransmission and the Markov chain changes to one-dimensional, the transmission probability can be expressed as the same with the transmission probability equation derived from the 1-D Markov chain under saturated condition in [6]. That is

$$\tau = \frac{2-2p}{1-2p+w_0}. \tag{42}$$

If we set $m = 1$ and $f = \infty$, i.e., the contention window size is limited to be doubled only once upon a retransmission and then stays constantly at the double value even if retransmissions still happen later. Moreover, packets are permitted to be retransmitted until successful reception by the receiver, we have

$$\tau = \frac{2-2p}{1-2p+w_0+w_0 q}. \tag{43}$$

In (43), given the density profile, the busy channel probability p is a function of τ_{R_I} from (21). w_0 is a constant of which the value is decided by the EDCA setting. As a result, τ is a function of the collision probability q. In this thesis, for simplicity, we use (43) as the expression for the transmission probability of the car at location a, which is a function of collision probability for the packet transmitted from car a. The expression (43) furnishes a relationship between the transmission probability τ and the collision probability q.

Chapter 5 The Interference Model for Transmissions

In this chapter, an interference model is proposed to investigate packet collisions in different regions. Section 5.1 gives a general overview of interference and illustrates with an example. We analyze the possible interference regions piecewisely in Section 5.2 and particularly we specify the cases for hidden nodes in the last region. Finally, Section 5.3 summarizes all the interference regions to obtain the expression of collision probability for the transmission from a car as a function of transmission probability. The computation for obtaining the values of transmission probability and collision probability is also presented in the last section.

5.1 The General Interference Scenario

Based on the vehicular density profile $n(x)$ as the input from the stochastic traffic model, interference engendered by transmitting vehicles in V2V communications is modeled to identify the packet collision probability of a car as a function of the corresponding transmission probability. To start with, the scenario of the interference should be firstly exhibited. Vehicles normally transmit and receive through generally two types of antennas, they are respectively the omnidirectional antenna and the directional antenna. Omnidirectional antenna [33] radiates and receives electromagnetic wave power uniformly in all directions on one plane. A directional antenna [34] is an antenna which radiates and receives greater wave power in specific directions so that there is amplification for transmitted power and received power, while the interference from unwanted sources is abated. In this thesis, the use of omnidirectional antenna is assumed. Therefore, a car which is receiving packets will be interfered by transmitting vehicles within its sensing range (or interference range) no matter which direction they transmit to. For simplicity, here we only consider the data transmission on the backward direction as drivers commonly care more about the preceding cars. The forward transmission can be analyzed similarly.

Figure 5.1 illustrates the interference scenario for the backward transmission of packets from a given car at location a (let us denote it as car a for simplicity). For an ongoing unicast transmission from car a to a car at location x (car x) located within the transmission range R_S (which has been set with the sensing/interference range R_I in Chapter 4), if there is at least one more car such as the car at location b, c, d or e (car b, c, d or e) which transmits and is located within the sensing range R_I of car x, then it interferes with the signal reception at car x, or collision happens at car x. Here, the transmitting car b, c, d and e are called interference sources or interferers for the transmission from the sender a to the receiver x. The Interferers are possibly located in any locations within the sensing range of the receiver x, and all the possible locations of the interferers can be divided into four non-overlapping regions: $[a - R_S, a)$, $(a, x + R_I]$, $[a - R_I, a - R_S)$ and $[x - R_I, a - R_I)$. Note that as x varies within $[a - R_S, a)$, the regions $(a, x + R_I]$ and $[x - R_I, a - R_I)$ will vary accordingly. Car b is an example for interferers in Region 1 $[a - R_S, a)$. Interferer c is an example in Region 2 $(a, x + R_I]$. Car d and e are the interferer examples in Region 3 $[a - R_I, a - R_S)$ and Region 4 $[x - R_I, a - R_I)$ respectively. We model the interference by analyzing the four regions of interferers and their effect on the transmission of car a. This analysis will provide us the interference probability in every one of the four regions aforesaid, and we finally synthesize all the interference probability to obtain another relationship between the collision probability q and the transmission probability τ besides the relationship which has been found in the previous chapter. Combining the two relationships, values of transmission probability and collision probability can be computed.

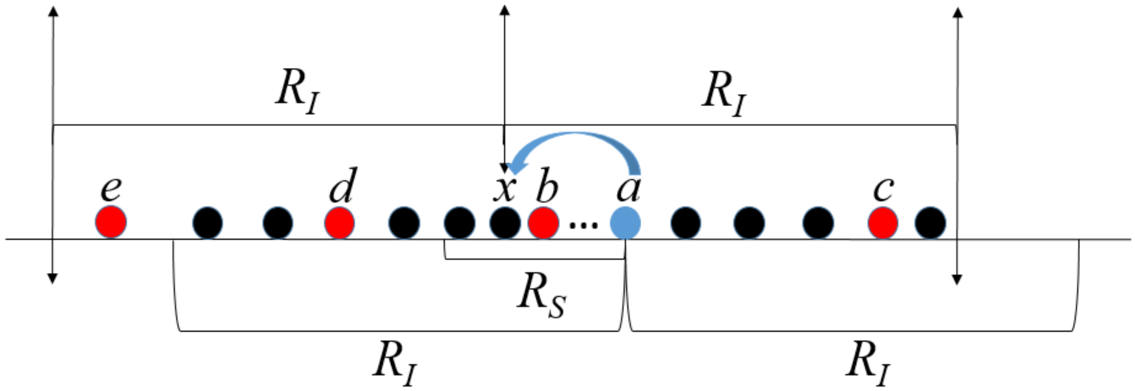

Figure 5.1. The interference scenario.

5.2 The Four Interference Regions

From now on, we go through the analysis for the four non-overlapping interference regions one by one to find the respective interference probability from each region, given the density profile $n(x)$. Before moving to the analysis, we assume that cars arrive according to a Poisson process, then the probability that there are i cars in car a's the transmission range $[a - R_S, a)$ is

$$P\{i \text{ cars in } [a - R_S, a)\} = \frac{\bar{N}_{R_S}{}^{i} e^{-\bar{N}_{R_S}}}{i!}, \tag{44}$$

where $0 \leq i < +\infty$ and $\bar{N}_{R_S} = \int_{a-R_S}^{a} n(x)dx$ according to (17) or (18) is the mean number of cars in the transmission range R_S of car a. We also assume that the i cars in transmission range $[a - R_S, a)$ have equal probability to be randomly chosen as the receiver of the unicast from car a, i.e., if we sort the i cars from 1 to i, the k-th car chosen as the receiver has the probability

$$P(k) = \frac{1}{i}, \tag{45}$$

where $1 \leq k \leq i$.

5.2.1 Interferers in Region 1: [a – R_S, a)

If there is at least one interferer in this region, the packet reception at car x will be ruined wherever the interferers are located. It is noteworthy that if the receiver x transmits simultaneously when it receives the packet from car a, the packet reception will also fail. Thus, if there are i cars in $[a - R_S, a)$, the probability that there is at least one car such as car b transmitting in Region 1 can be expressed as

$$B = 1 - \left(1 - \tau_{R_S}\right)^i, \tag{46}$$

where τ_{R_S} is the average transmission probability of cars in Region 1. When car a transmits, the probability that the receiver (the k-th car) among the i cars in $[a - R_S, a)$ is interfered by the transmitting cars in Region 1 is then reaped from (45) and (46) as

$$P_{Intf1}(k) = P(k)B. \tag{47}$$

Every one of all cars from k=1 to k=i in the transmission range $[a - R_S, a)$ is possibly chosen as the receiver. So the probability for all possible receivers of the packet transmission from car a be interfered can be summarized from (47) as

$$\sum_{k=1}^{i} P(k)B = \sum_{k=1}^{i} P_{Intf1}(k). \tag{48}$$

The probability for existence of i cars in region $[a - R_S, a)$ is given by (44). Hence, the interference probability from Region 1 can be obtained as $P\{i \text{ cars in } [a - R_S, a)\} \sum_{k=1}^{i} P_{Intf1}(k)$. Theoretically, the number of cars i in car a's transmission region $[a - R_S, a)$ can range from 0 to infinity. Therefore, we have the overall interference probability from Region 1 by combining (44) to (48) with the Taylor formula as follows,

$$\begin{aligned} P_1 &= \sum_{i=1}^{\infty} P\{i \text{ cars in } [a - R_S, a)\} \sum_{k=1}^{i} P_{Intf1}(k) \\ &= \sum_{i=1}^{\infty} \frac{\bar{N}_{R_S}{}^{i} e^{-\bar{N}_{R_S}}}{i!} \sum_{k=1}^{i} \frac{1}{i} \left[1 - \left(1 - \tau_{R_S}\right)^i\right] \\ &= 1 - e^{-\tau_{R_S} \bar{N}_{R_S}}. \end{aligned} \tag{49}$$

5.2.2 Interferers in Region 2: (a, x+R_I]

In this case, whether the packet reception at car x is ruined depends on whether there is any car transmitting in Region 2. Let $C(x)$ be the probability that at least one car e.g. car c transmits in Region 2. As the cars are Poisson distributed in Region 2, specifically we have the following expression with the Taylor formula,

$$
\begin{aligned}
C(x) &= 1 - \sum_{n=0}^{\infty} P(n \text{ cars in Region 2}) P(n \text{ cars do not transmit}) \\
&= 1 - \sum_{n=0}^{\infty} \frac{\overline{N}_C(x)^n e^{-\overline{N}_C(x)}}{n!} (1-\tau_C)^n \\
&= 1 - e^{-\tau_C \overline{N}_C(x)},
\end{aligned} \tag{50}
$$

where $\overline{N}_C(x) = \int_a^{x+R_I} n(s)ds$ and τ_C are the average number of cars in Region 2 and the average transmission probability of cars in this region, respectively. According to [3], given the vehicular density profile $n(x)$, we can identify the probability density function (PDF) $f(x)$ for a car located at x within the transmission range $[a–R_S, a)$ of car a as follows,

$$
f(x) = \begin{cases} \dfrac{n(x)}{\overline{N}_{R_S}}, a - R_S \le x < a \\ 0, \qquad\qquad \text{otherwise} \end{cases}. \tag{51}
$$

Thus, from (45) and (51), the PDF for the k-th one of i cars in $[a - R_S, a)$ located on x is $P(k)f(x)$. As x can be any location in $[a - R_S, a)$, the probability that the k-th car located at x varying in $[a - R_S, a)$ is interfered by transmitting cars in Region 2 is derived by integrating the foregoing PDF $P(k)f(x)$ with $C(x)$ from (50) as

$$
P_{Intf2}(k) = P(k) \int_{a-R_S}^{a} f(x)C(x)dx. \tag{52}
$$

Similar to (49) in Region 1, the overall interference probability from Region 2 can be acquired by combining (44), (45), (50), (51) and (52) as follows,

$$
\begin{aligned}
P_2 &= \sum_{i=1}^{\infty} P\{i \text{ cars in } [a - R_S, a)\} \sum_{k=1}^{i} P_{Intf2}(k) \\
&= \sum_{i=1}^{\infty} \frac{\overline{N}_{R_S}{}^{i} e^{-\overline{N}_{R_S}}}{i!} \sum_{k=1}^{i} \frac{1}{i} \int_{a-R_S}^{a} \frac{n(x)}{\overline{N}_{R_S}} [1 - e^{-\tau_C \overline{N}_C(x)}] dx \\
&= \frac{1 - e^{-\overline{N}_{R_S}}}{\overline{N}_{R_S}} \int_{a-R_S}^{a} n(x)[1 - e^{-\tau_C \overline{N}_C(x)}] dx.
\end{aligned} \tag{53}
$$

5.2.3 Interferers in Region 3: [a–R_I, a–R_S)

If at least one car in this region transmits at the same time car x receives the packet from car a, the transmission from car a will be interfered. Let D be the probability that at least one car for example car d transmits in Region 3. Similar to (50) in Region 2, we have

$$\begin{aligned} D &= 1 - \sum_{n=0}^{\infty} P(n \text{ cars in Region } 3) P(n \text{ cars do not transmit}) \\ &= 1 - \sum_{n=0}^{\infty} \frac{\bar{N}_D{}^n e^{-\bar{N}_D}}{n!} (1-\tau_D)^n \\ &= 1 - e^{-\tau_D \bar{N}_D}, \end{aligned} \tag{54}$$

where $\bar{N}_D = \int_{a-R_I}^{a-R_S} n(s)ds$ and τ_D are the average number of cars in Region 3 and the average transmission probability of cars in the region, respectively. Resembling the expression (52), with (45), (51) and (54), the probability that the k-th car located at x in [a – R_S, a) is interfered by cars in Region 3 is given by

$$P_{Intf3}(k) = P(k) D \int_{a-R_S}^{a} f(x)dx. \tag{55}$$

Then, by combining (44), (45), (51), (54) and (55), the overall interference probability from Region 3 is obtained as follows,

$$\begin{aligned} P_3 &= \sum_{i=1}^{\infty} P\{i \text{ cars in } [a-R_S, a)\} \sum_{k=1}^{i} P_{Intf3}(k) \\ &= \sum_{i=1}^{\infty} \frac{\bar{N}_{R_S}{}^i e^{-\bar{N}_{R_S}}}{i!} \sum_{k=1}^{i} \frac{1}{i} (1 - e^{-\tau_D \bar{N}_D}) \int_{a-R_S}^{a} \frac{n(x)}{\bar{N}_{R_S}} dx \\ &= \frac{(1-e^{-\bar{N}_{R_S}})(1-e^{-\tau_D \bar{N}_D})}{\bar{N}_{R_S}} \int_{a-R_S}^{a} n(x)dx. \end{aligned} \tag{56}$$

5.2.4 Interferers in Region 4: [x–R_I, a–R_I)

The packet reception at car x will be ruined if there is at least one interferer in this region. Let $E(x)$ be the probability that at least one car such as car e transmits in Region

4, we have

$$E(x) = 1 - \sum_{n=0}^{\infty} P(n \text{ cars in Region 4}) P(n \text{ cars do not transmit})$$
$$= 1 - \sum_{n=0}^{\infty} \frac{\overline{N}_E(x)^n e^{-\overline{N}_E(x)}}{n!} (1 - \tau_E)^n$$
$$= 1 - e^{-\tau_E \overline{N}_E(x)}, \quad (57)$$

where $\overline{N}_E(x) = \int_{x-R_I}^{a-R_I} n(s)ds$ and τ_E are the average number of cars in Region 4 and the average transmission probability of cars in the region, respectively.

What should be noted is that, from Figure 5.1, all interferers are located beyond the sensing range of car *a*, and they are actually the hidden nodes for the transmission from car *a* to car *x*. The hidden nodes can also cause interference to car *x*. In Region 4, there are three cases for the transmission of hidden nodes as follows.

Case 1: as shown in Figure 5.2, hidden nodes transmit at the same time node *a* transmits, resulting in concurrent transmissions.

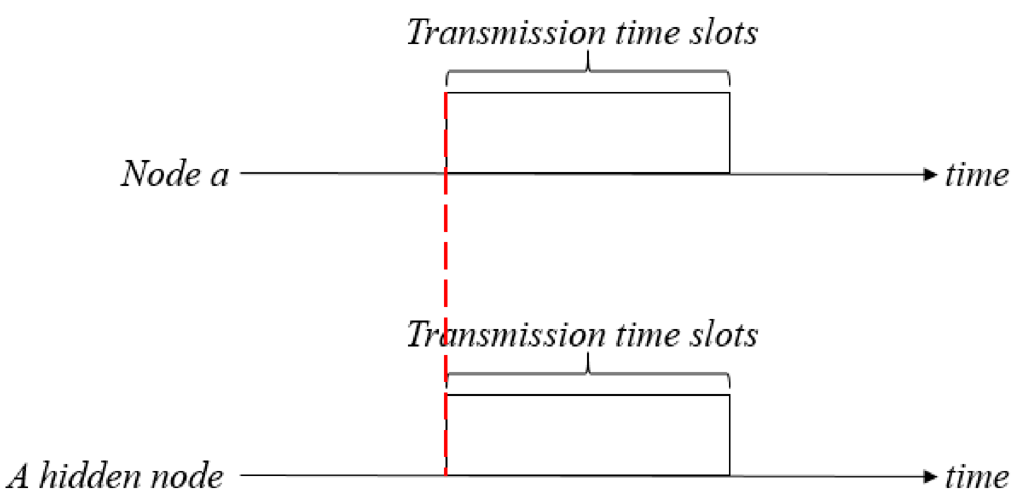

Figure 5.2. Case 1 for the transmission of hidden nodes.

Case 2: as shown in Figure 5.3, hidden nodes transmit before the transmission of node *a*.

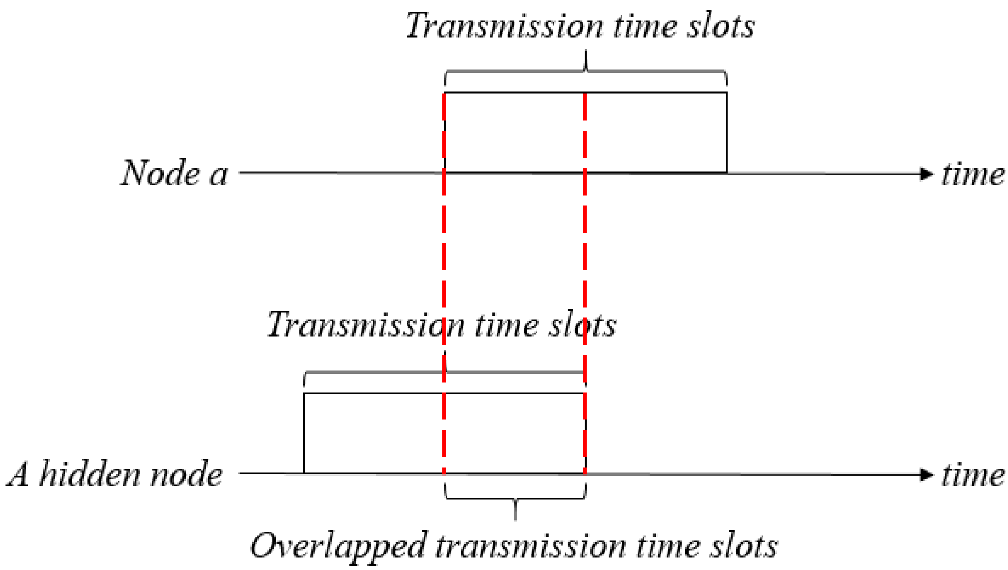

Figure 5.3. Case 2 for the transmission of hidden nodes.

Case 3: as shown in Figure 5.4, node *a* transmits first, then hidden nodes transmit.

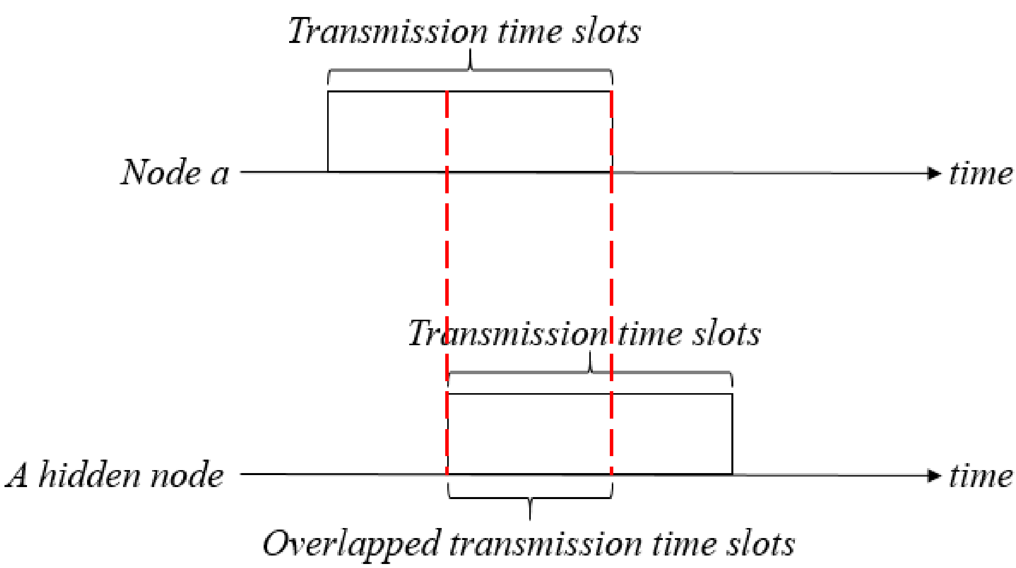

Figure 5.4. Case 3 for the transmission of hidden nodes.

We can see that, although hidden nodes and car *a* do not start transmitting concurrently in case 2 & 3, there still exist some overlapped transmission time slots as hidden nodes or car *a* begin to transmit in the midst of the transmission duration of each other.

For case 1 & 2, considering from the time slot at which car *a* initiates the transmission, we can derive the conditional probability that the *k*-th car in car *a*'s transmission range $[a - R_S, a)$ chosen as the receiver located at x is interfered by transmitting nodes in Region 4 by combining (45), (51) and (57) as follows, which is similar to (52) in Region 2.

$$P_{Intf4\_1}(k) = P(k)\int_{a-R_S}^{a} f(x)E(x)dx. \tag{58}$$

For case 3, we still consider from the time slot when car a commences its transmission, and the state (contending or transmitting) of each node is considered in every expected time slot $pT + (1 - p)$ (which has been stipulated for the Markov chain in Chapter 4). Let J be the number of expected slots needed to complete one practical transmission time of T physical slots. Then the hidden nodes will probably start transmitting at any one of the expected time slots of car a's transmission duration from the 2nd slot to the J-th slot ($J \geq 2$). If the hidden nodes start transmitting at the 2nd expected time slot of car a's transmission interval, it means there is no car transmitting at the 1st expected time slot with the probability $1 - E(x)$ from (57), the probability that at least one hidden node transmits at the 2nd expected time slot in Region 4 can be given by

$$P_{exp}(1) = [1 - E(x)]E(x). \tag{59}$$

Similarly, the probability that at least one hidden node transmits at the 3rd expected time slot in Region 4 can be expressed as

$$P_{exp}(2) = [1 - E(x)]^2 E(x). \tag{60}$$

By parity of reasoning, we can conclude the probability that at least one hidden node transmits at the (j+1)-th expected time slot in Region 4 as follows.

$$P_{exp}(j) = [1 - E(x)]^j E(x), \tag{61}$$

where $1 \leq j \leq J - 1$. By summation of the probability (61) that at least one hidden node transmits from the 2nd expected time slot (j = 1) to the J-th expected time slot ($j = J$ - 1) foresaid and combining (45) and (51), the conditional interference probability from Region 4 in case 3 can be expressed as

$$P_{Intf4\_2}(k) = P(k)\int_{a-R_S}^{a} f(x)\sum_{j=1}^{J-1} P_{exp}(j)\, dx. \tag{62}$$

Therefore, by summation of the conditional interference probability (58) and (62) for the three cases above and combining (44), (45), (51), (57) and (61), the overall interference probability from Region 4 is summarized as

$$P_4 = \sum_{i=1}^{\infty} P\{i \text{ cars in } [a - R_S, a)\} \sum_{k=1}^{i} [P_{Intf4\_1}(k) + P_{Intf4\_2}(k)]$$

$$= \sum_{i=1}^{\infty} \frac{\bar{N}_{R_S}{}^{i} e^{-\bar{N}_{R_S}}}{i!} \sum_{k=1}^{i} \{\frac{1}{i}\int_{a-R_S}^{a} \frac{n(x)}{\bar{N}_{R_S}} [1 - e^{-\tau_E \bar{N}_E(x)}] dx + \frac{1}{i}\int_{a-R_S}^{a} \frac{n(x)}{\bar{N}_{R_S}} \sum_{j=1}^{J-1} [e^{-\tau_E \bar{N}_E(x)}]^j [1 - e^{-\tau_E \bar{N}_E(x)}]\, dx\}$$

$$= \frac{1 - e^{-\bar{N}_{R_S}}}{\bar{N}_{R_S}} \int_{a-R_S}^{a} n(x) \left[1 - e^{-\tau_E \bar{N}_E(x)}\right] [1 + \sum_{j=1}^{J-1} e^{-j\tau_E \bar{N}_E(x)}] dx. \tag{63}$$

The expression (63) above shows the effect of the hidden nodes for the backward transmission. Note that if we also incorporate the forward transmission into the interference model, the interference probability from Region 4 will be higher as the hidden nodes' effect will be more significant.

5.3 Collision Probability

Now we determine J in (63) for finally deriving the expression of collision probability q for packets transmitted from car a with a given density profile $n(x)$ from the stochastic traffic model. From the definition of J aforesaid in Section 5.2.4, we have

$$J = \left\lceil \frac{T}{pT + 1 - p} \right\rceil. \tag{64}$$

Note that $T/(pT + 1 - p)$ is normally a fractional number, but J must be an integer. So if $T/(pT + 1 - p)$ is not an integer, we set J as the smallest integer greater than $T/(pT + 1 - p)$ (e.g. if the result is 2.1, set J as 3). As T is a constant value, the number J of expected slots which can accommodate one practical transmission time T only hinges on the channel busy probability p. Thus, J can be predetermined with only case 1 and case 2 (without case 3) for the transmission of hidden nodes in Region 4 by the predetermined channel busy probability p'. Combining (44), (45), (51), (57) and (58), the predetermined overall interference probability from Region 4 with only cases 1 & 2 can be defined as

$$P_4{}' = \sum_{i=1}^{\infty} P\{i \text{ cars in } [a - R_S, a)\} \sum_{k=1}^{i} P_{Intf4\_1}(k)$$

$$= \sum_{i=1}^{\infty} \frac{\bar{N}_{R_S}{}^{i} e^{-\bar{N}_{R_S}}}{i!} \sum_{k=1}^{i} \frac{1}{i} \int_{a-R_S}^{a} \frac{n(x)}{\bar{N}_{R_S}} \left[1 - e^{-\tau_E \bar{N}_E(x)}\right] dx$$

$$= \frac{1 - e^{-\bar{N}_{R_S}}}{\bar{N}_{R_S}} \int_{a-R_S}^{a} n(x)\left[1 - e^{-\tau_E \bar{N}_E(x)}\right] dx. \quad (65)$$

Then, by combining (49), (53), (56) and (65), the predetermined collision probability by all four interference regions with only case 1 and 2 for Region 4 can be expressed as

$$q' = 1 - (1 - P_1)(1 - P_2)(1 - P_3)(1 - P_4'). \quad (66)$$

Let τ_{Intf} be the average transmission probability for the cars within the whole interference area [a - R_S - R_I, a + R_I] for the transmission from car a, and we approximately preset all transmission probability mentioned in Chapter 4 & 5 within this area as τ_{Intf}, that is

$$\tau = \tau_{R_I} = \tau_{R_S} = \tau_C = \tau_D = \tau_E = \tau_{Intf}. \quad (67)$$

Thus, all interference probability can be replaced with τ (the transmission probability of car a) for preliminary solution of equations. Then, with a given density profile $n(x)$, q' is a function of one and only variable τ' in (66) (here, we use τ' as a predetermined value) and τ' is a function of a single variable q' in (43). We couple (66) with (43) for solving the two equations to obtain the values of predetermined transmission probability τ' and the predetermined transmission probability q'. By substituting the value τ' into (21), the predetermined channel busy probability value p' is derived, and then we can have the predetermined value J' from (64). With the predetermine value J', the overall interference probability P_4 in (63) can be decided. Eventually, combining (49), (53), (56) and (63), we can conclude the collision probability for the transmission from car a to car x which is substantially the probability that interferers exist in at least one of the four interference regions as follows,

$$q = 1 - (1 - P_1)(1 - P_2)(1 - P_3)(1 - P_4). \quad (68)$$

We can see that (68) offers another relationship between the collision probability q and the transmission probability τ besides (43), and q is a function of the sole variable τ using the presetting in (67). Associating (68) with (43), (21) and (64), we can get the updated values of τ, q, p and J compared with the predetermined ones. If updated J is equal to predetermined J', i.e., $J = J'$, the updated values of τ and q can be the finalized values. Otherwise, we set updated J as the new predetermined value instead of J' for (63) and repeat the computation of (68) and (43) to find the 2nd-round updated values of τ, q, p and J with (21) and (64). We iterate the comparison between updated J and the predetermined one in every round to finally determine the value of J, and iterate computation of (68) and

(43) if necessary to find the finalized values of τ and q for car a. Note that the finalized values here are actually the approximated values of τ and q according to (67).

We can get approximated τ and q at every location on the traffic road in the same manner foresaid, and then we can also iteratively deduce the specific values of τ_{R_I}, τ_{R_S}, τ_C, τ_D and τ_E by approximated τ at homologous locations without using the presetting in (67) to derive the more precise values of τ and q by iterative computation of (68) and (43) with accordingly adjusting the value of J determined before with (21) and (64), until the results with satisfactory precision are found. The flow chart for the whole computation process for transmission probability and collision probability is illustrated in Figure 5.5.

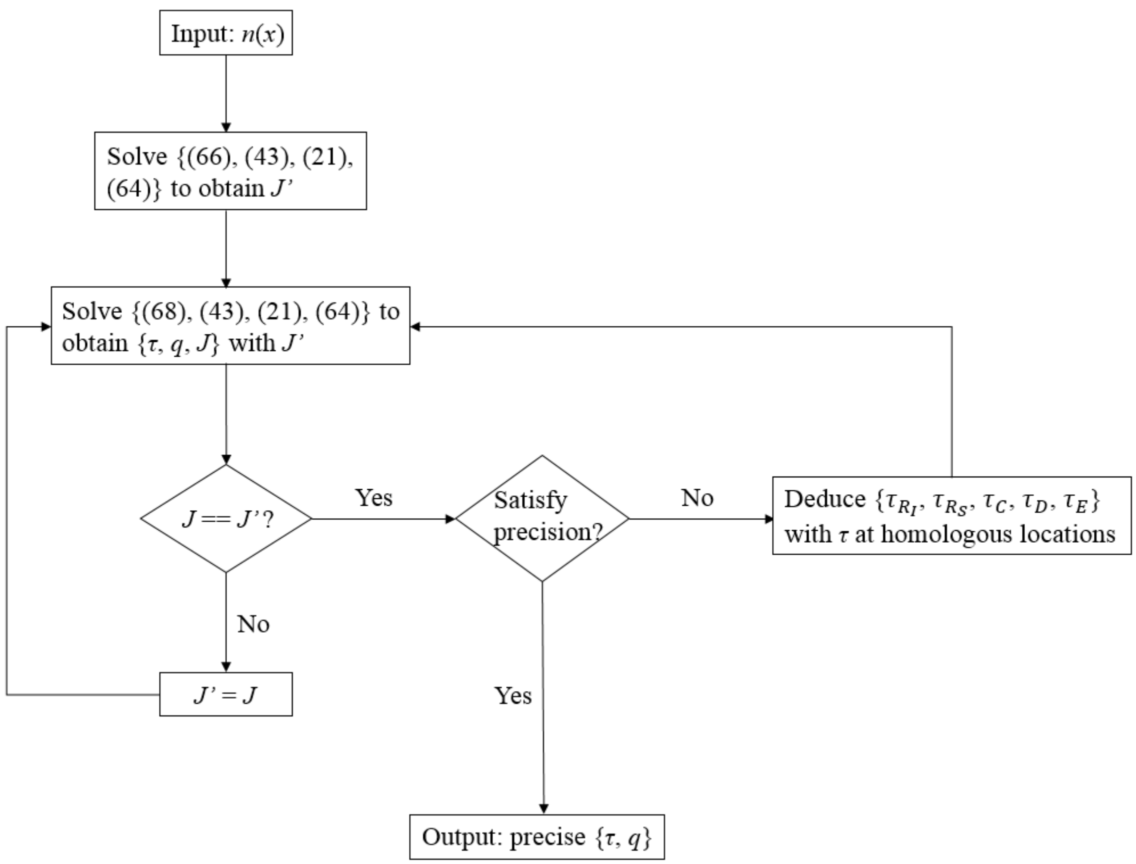

Figure 5.5. The computation process for transmission probability and collision probability.

Chapter 6 The Performance Model

In this chapter, the performance model for deriving the transmission delay and throughput of a car at any location on a road segment for V2V communications is established based on the Markov chain for single access class queue in Chapter 4, given the inputs which are the car's transmission probability and collision probability obtained from the coalescence of the contention model in Chapter 4 and the interference model in Chapter 5.

The unicast delay is defined as the duration from the beginning of contention to access the channel for packet transmission to the time that the ACK for that packet is received by the transmitter for confirmation of successful packet reception. Hence, the delay includes contention time for the packet to access the channel, transmission time for the packet loaded onto the channel from the transmitting node, propagation time for the packet transmitted from the source to the destination and the acknowledgement delay. The signal propagation time (the distance between the sender and the receiver within the transmission range of the sender/ speed of light) is neglected, as we assume that the transmission range of each vehicle is at most 500 m. According to [10], once a node receives a packet, it will transmit the ACK for the packet to the sender after a Short Inter-Frame Space (SIFS). In line with the 2-D Markov chain (in Chapter 4) for medium access process, Figure 6.1 illustrates the unicast delay for a packet which consists of zero or a sequence of failed transmission intervals incurred by collisions and a successful transmission interval at last if there is no collision. A successful transmission interval consists of a contention duration, a transmission duration, a SIFS and an ACK transmission duration, while a failed transmission interval merely comprises a contention duration and a transmission duration without the ACK sent back from the receiver.

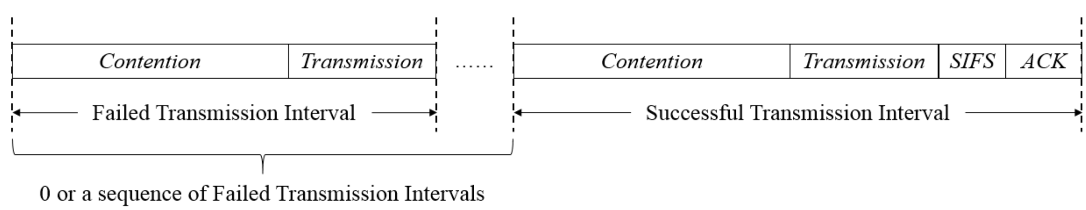

Figure 6.1. Unicast delay for a packet transmitted from a car.

A contention duration mentioned above can be considered as a number of expected time slots of which each is $pT + (1 - p)$ based on the Markov chain. Here, T is a constant which denotes a transmission duration (the packets size/ data rate). The contention duration is equal to i expected time slots before the car transmits, with the probability

$$P(a\ contention\ duration = i * expected\ time\ slot) = (1-\tau)^i\tau, \tag{69}$$

where τ is the transmission probability of the car. The expression (69) purports that the car does not transmit until the (i+1)-th expected time slot. From (69), we can see that

$$\sum_{i=0}^{\infty} P(a\ contention\ duration = i * expected\ time\ slot) = \sum_{i=0}^{\infty}(1-\tau)^i\tau = 1, \tag{70}$$

where $0 < \tau < 1$. Then in light of [6], with (70), the expected contention duration in the back-off stage of the Markov chain is given by

$$\begin{aligned}\overline{CT} &= \sum_{i=0}^{\infty} i[pT + (1-p)]P(a\ contention\ duration = i * expected\ time\ slot)\\ &= \sum_{i=0}^{\infty} i[pT + (1-p)](1-\tau)^i\tau\\ &= \left(\frac{1}{\tau} - 1\right)(pT + 1 - p).\end{aligned} \tag{71}$$

From Figure 6.1, obviously a failed transmission interval is

$$T_C = \overline{CT} + T. \tag{72}$$

A successful transmission interval is

$$T_S = \overline{CT} + T + SIFS + ACK. \tag{73}$$

Then, the delay D can be summarized from (72) and (73) as

$$D = nT_C + T_S, \text{where } n \geq 0. \tag{74}$$

The probability that there are n occurrences of collisions before a successful transmission is expressed as

$$P(n\ collisions) = q^n(1-q), \tag{75}$$

where q is the collision probability. Similar to (70), we can get the following expression by summation of (75) that

$$\sum_{n=0}^{\infty} P(n\ collisions) = \sum_{n=0}^{\infty} q^n(1-q) = 1, \tag{76}$$

where $0 < q < 1$. For brevity of computation, the SIFS and the ACK transmission duration are left out. Finally we combine (71) to (76) to derive the expected unicast delay for a packet transmitted by a car as follows,

$$E[D] = \sum_{n=0}^{\infty} D * P(n\ collisions)$$
$$= \sum_{n=0}^{\infty} [n(\overline{CT} + T) + (\overline{CT} + T)] * q^n(1-q)$$
$$= \frac{1}{1-q}\left[\left(\frac{p}{\tau} - p + 1\right)T + \left(1 - \frac{1}{\tau}\right)p + \frac{1}{\tau} - 1\right]. \quad (77)$$

As the values of the transmission probability τ, the collision probability q and the busy channel probability p for a car can be found from the contention model and the interference model (in the previous two chapters), we can compute the expected unicast delay with these values.

After reaping the expected delay from (77), we can easily compute the expected throughput of a car, dividing the packet size L by the expected delay for the packet as follows,

$$E[\rho] = \frac{L}{E[D]}. \quad (78)$$

Chapter 7 The Cross-layer Optimization

This chapter presents a cross-layer optimization method on both the PHY layer and MAC layer. Section 7.1 gives the pandect of the optimization which sketches out the general optimization approaches. The PHY-layer optimization scheme and the MAC-layer optimization algorithm are expatiated in Section 7.2 and Section 7.3 respectively.

7.1 The Overview of Optimization

The interference range strongly influences the network performance, as senders sense the channel within their own interference range before transmitting packets and receivers also suffer from collisions on packet reception by concurrent transmissions or the hidden-node corruption within the interference range. From [24, 35], a vehicle's transmission range R_S is closely tied to the interference range R_I which will expand or shrink abiding by the corresponding adjustment of the transmission range, and the relationship between the transmission range and the interference range follows

$$R_I = \beta^{\frac{1}{\alpha}} R_S, \tag{79}$$

where β is the signal-to-interference ratio (SIR) requirement and α is the path-loss exponent with $\alpha > 2$. Thereby, the power control adjusting the transmission range can accordingly tune up the interference range for PHY-layer optimization to improve the network performance.

Some limitations of 802.11p MAC exist in accordance with [21]. The internal collisions on packet transmissions within a node can be prevented by the scheme through granting the transmission opportunity (TXOP) to the highest-priority service, but the external collisions cannot be avoided. Additionally from [26], there are deficiencies for using a fixed contention window size on all vehicles in unicast. In a dense network, vehicles will have an insufficient back-off period, hence increasing the chance of collisions. On the other hand, vehicles will gratuitously wait too long for the back-off in the case of a sparse network, causing mediocre bandwidth utilization. Therefore, the congestion control approach for MAC-layer optimization is to assign varying contention window sizes for vehicles at different locations according to the vehicular density in vicinity to drop external collision probability, meanwhile guarantee efficient utilization of bandwidth.

The holistic modeling (foresaid from Chapter 3 to Chapter 6) including the stochastic traffic model and the network model (the contention model, the interference model, and the performance model) provides predictable evolution of the vehicular density and network performance. Based on the modeling, this thesis proposes a novel cross-layer optimization method on both the PHY layer and MAC layer in V2V communications without continuously monitoring and measuring vicinal network loads to identify the optimal transmission range and the optimal contention window size on every location, given the velocity profile as the input as shown in Figure 1.1. Then individual vehicle can set its transmission range and contention window size to the optimal values adaptively according to its location known from the equipped GPS device or RSUs for optimizing the overall network performance.

7.2 The PHY-layer Optimization

We now study the optimization on PHY layer to decide the optimal transmission ranges of vehicles at different locations, given the density profile as the input. Network performance can be optimized through dwindling the transmission range and then the interference range of each car, but in the meantime the network connection should also be ensured to prevent network fragmentation. In this thesis, the 1-D traffic is considered (in Chapter 3). From [3], one node is connected to one of its forward nodes on the right on the 1-D road if the distance d between them is less than or equal to the transmission range R_S of the forward node, that is $d \leq R_S$. Then, the network in the 1-D traffic is defined to be connected if and only if there does not exist any node which is disconnected to any of its forward nodes ($d > R_S$). We can further classify the degree of connectivity which represents the number of direct single-hop neighbors a node has within the transmission range. Obviously, the degree of connectivity equal to 1 (1-*connectivity*) when a node gets only one single-hop neighbor, and this provides the minimum required transmission range (interference range) to ensure network connectivity and optimize the network performance. Further communications among the vehicular nodes can be realized by forwarding the packets through multi-hop routing.

Based on the density profile $n(x)$ from the stochastic traffic model, we have the following expression for a vehicle at location a in a 1-*connected* network that

$$\int_{a-R_{1con}}^{a} n(x)dx = 1, \tag{80}$$

where R_{1con} is the transmission range within which there is one car on average. As $n(x)$ is the mean density, the expression (80) has no means to ensure the network is connected. So, the optimal transmission range R_{op} which ensures the network connection and promotes network performance can be decided as

$$R_{op} = R_{1con} + \delta, \tag{81}$$

where δ is an offset parameter. The value of δ increases from 0 to 0.1 by every 0.01 ($\delta = \{0, 0.01, 0.02 \ldots 0.1\}$), so there are totally eleven optional values for δ. We divide the road region [0, 4] km into units with 0.01 km for each unit, and implement the simulation for each δ based on the simulation framework which is stated in the next chapter to output result '1' if the network is connected in a unit, or result '0' if the network is disconnected in the unit. We run 3000 rounds of simulation for one δ to guarantee a satisfactory accuracy. For every δ, after running 3000 rounds of simulation, there is a percentage of connected occurrences in one unit that

$$P(\text{con}) = \frac{\sum \text{occurences of result 1}}{\sum \text{occurences of result 1 \& 0}}. \tag{82}$$

If P(con) is not lower than a predetermined probability threshold 0.8 (This is a tradeoff value: if we set the threshold too high, the transmission range will be very large which cannot optimize the network performance with the default transmission range 0.2 km; if we set the threshold too low, the transmission range obtained cannot ensure the network connectivity.), i.e., $P(\text{con}) \geq 0.8$, the network connection can be thought to be ensured. Then δ can be used and the optimal transmission range R_{op} at the location can be determined. Using this method, the optimal transmission range at every location can be found.

7.3 The MAC-layer Optimization

As discussed in Section 7.1, the optimal contention window size on every location should be found to control the channel access contention for the optimization in the MAC layer based on the network model and the stochastic traffic model. Figure 7.1 indicates the analytical distributions of delay and throughput at different contention window sizes for single access class queue in homogeneous traffic with different vehicular density from 5 cars/km to 30 cars/km, which are computed through the established network model, given R_S = 0.2 km, R_I = 0.5 km and other parameters' values according to Table 8.1. We can see that from the contention window size w = 4 to w = 512, the delay for all vehicular density firstly decreases (throughput increases) because there will be longer waiting time for avoidance of collisions as w increases, and then the delay increases (throughput decreases) if w is much larger than the adequate waiting time for averting collisions. So the performance curves are unimodal and the optimal contention window size w_{op} must be within the interval [4, 512]. w_{op} will become larger when density increases as longer contention time is demanded for more vehicles in traffic to diminish collisions, while it will lessen to retrench unwanted waiting time before the transmission when density decreases.

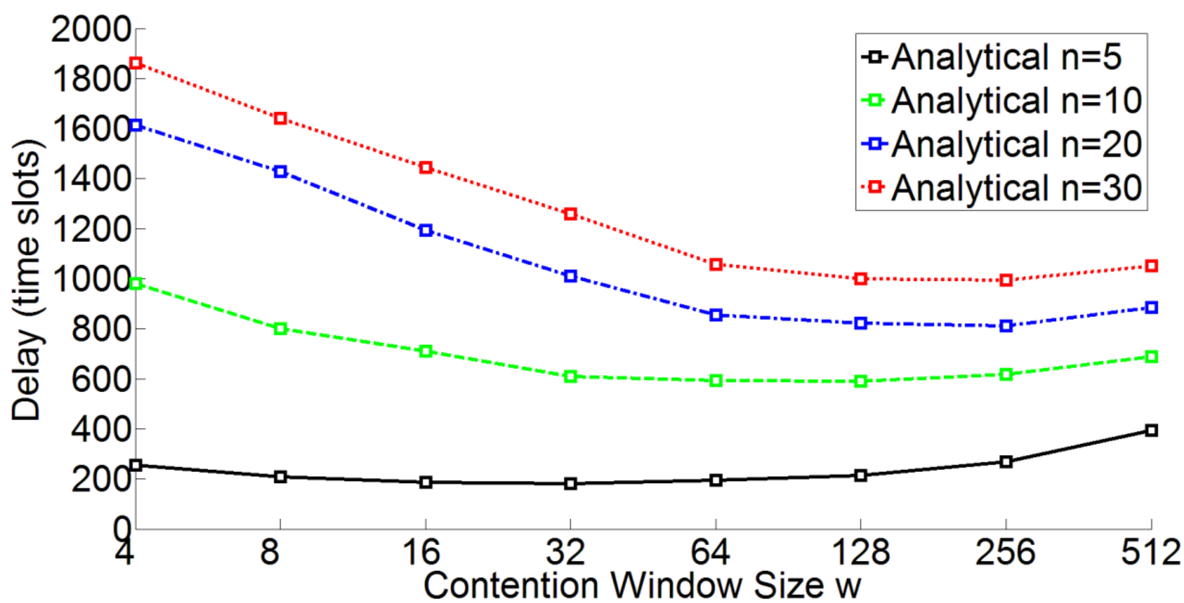

a) Delay

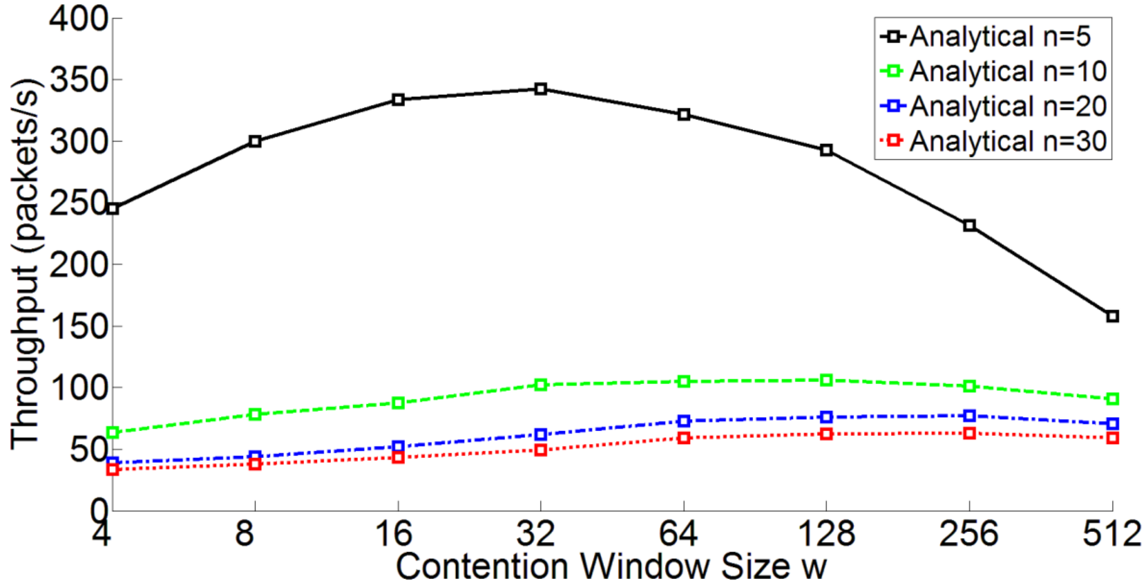

b) Throughput

Figure 7.1. Analytical performance against the contention window size *w* for homogeneous traffic.

An algorithm for finding w_{op} within the range [4, 512] is developed for MAC-layer optimization at every location in heterogeneous traffic by the network modeling based on the stochastic traffic model as follows.

Step 1: Find the minimal delay D_m at contention window size w_m from w = {4, 8, 16, 32, 64, 128, 256, 512} with higher delay D_1 and D_2 at adjacent two contention window sizes $w_1 = w_m / 2$ and $w_2 = w_m * 2$ through the network model.

Step 2: Implement quadratic curve fitting for the three points (w_1, D_1), (w_m, D_m) and (w_2, D_2) in the coordinate system to obtain a provisional delay function of w: $D(w)$.

Step 3: Get the derivative of $D(w)$ to w, and let it equal to 0 for reaping a provisional optimal contention window size w_{op}.

Step 4: Check whether the provisional optimal contention window size from step 3 can make the delay minimum and iterate the optimal contention window size computation from step 2 to find the finalized minimal delay and the corresponding optimal contention window size as w_{op} through the network model.

The pseudocode of the MAC-layer optimization is shown in the following algorithm.

The MAC-layer Optimization Algorithm: Iterative Curve Fitting to find the Optimal Contention Window Size

Step 1:

```
for(w = 4; w <= 512; w = 2 * w)
{
 //Obtain the delay array from the computation of the analytical model.
 D[w] = Analytical model(density profile, transmission range, w);
 D[w * 2] = Analytical model(density profile, transmission range, w * 2);
 if(D[w / 2] > D[w] && D[w] < D[w * 2])
  {
   D_m = D[w];
   D_1 = D[w / 2];
   D_2 = D[w * 2];
   w_m = w;
   w_1 = w / 2;
   w_2 = w * 2;
   break;
  }
}
```

Step 2:

```
//Do curve fitting based on three delay points (w_1, D_1), (w_m, D_m), (w_2, D_2).
x = [w_1 w_m w_2];
y = [D_1 D_m D_2];
//Use quadratic polyfit to find the coefficients of polynomial a(1), a(2) and a(3)
a = polyfit(x, y, 2);
//Delay function of w: D(w) is obtained.
D(w) = a(1)w^2 + a(2)w + a(3);
```

Step 3:

$$\frac{dD(w)}{dw} = 0 \rightarrow 2a(1)w + a(2) = 0;$$

$$w_{op} = -\frac{a(2)}{2a(1)}; \text{ //round off}$$

Step 4:

```
/* iteratively determine the three delay value points for repeated curve fitting until the
   definitive optimal contention window size and delay in the range w ϵ [4, 512] are
   found. */
if(w_op == w_m)
 {
  D[w_m - 1]= Analytical model(density profile, transmission range, w_m - 1);
  D[w_m + 1] = Analytical model(density profile, transmission range, w_m + 1);
 if(D[w_m - 1] > D_m && D_m < D[w_m + 1])
  {
   D_op = D_m;
   Output result: w_op, D_op;  //The definitive optimal values are found.
   break; //Algorithm ends.
  }
 else if(D[w_m - 1] > D_m && D_m > D[w_m + 1])
 {
  w_1 = w_m;
  D_1 = w_m;
  w_m = w_m + 1;
```

```
   Dm = D[wm + 1];
  }
  else if(D[wm - 1] < Dm && Dm < D[wm + 1])
  {
   w2 = wm;
   D2 = wm;
   wm = wm - 1;
   Dm = D[wm - 1];
  }
  if(w1 == wm - 1 && w2 == wm + 1)
   {
    wop = wm;
    Dop = Dm;
    Output result: wop, Dop;  //The definitive optimal values are found.
    break; //Algorithm ends.
   }
  Iterate from Step 2;
  }

Dop = Analytical model(density profile, transmission range, wop);

if(Dop < Dm)
  {
  if(wop < wm)
   {
     w2 = wm;
     D2 = Dm;
     wm = wop;
     Dm = Dop;
   }
  else if(wop > wm)
   {
    w1 = wm;
    D1 = Dm;
    wm = wop;
    Dm = Dop;
   }
  if(w1 == wm - 1 && w2 == wm + 1)
   {
    Output result: wop, Dop;  //The definitive optimal values are found.
    break; //Algorithm ends.
   }
  Iterate from Step 2;
  }

else if(Dop > Dm)
{
  if(wop < wm)
   {
    w1 = wop;
    D1 = Dop;
   }
  else if(wop > wm)
   {
    w2 = wop;
    D2 = Dop;
```

```
    }
   if(w_1 == w_m - 1 && w_2 == w_m + 1)
    {
      w_op = w_m;
      D_op = D_m;
      Output result: w_op, D_op;  //The definitive optimal values are found.
      break; //Algorithm ends.
    }
  Iterate from Step 2;
 }
```

Finally, the cross-layer optimization can be carried out by firstly implementing the PHY-layer optimization to find the optimal transmission range at every location, and then implementing the MAC-layer optimization based on the different optimal transmission ranges on different locations to identify the optimal contention window size at every corresponding location. Note that, at different locations, the interference ranges of the potential receivers of a transmitter may be different as the optimal transmission ranges are possibly different, hence the interference regions in the interference model (discussed in Chapter 5) should be adjusted accordingly if the interference range of the receiver is different from that of the sender. Moreover, hidden nodes beyond the sensing range (interference range) of the transmitter could probably be able to sense the transmitter because those hidden nodes at their locations could have larger sensing ranges than the transmitter's after the transmission range adjustment. In such cases, case 3 for hidden nodes in the interference model will not take place and should be ignored for computing the collision probability of the packet transmission from the transmitter.

Chapter 8 Numerical Results

This chapter mainly presents the numerical results of our analytical model and the relevant simulation. Section 8.1 compactly introduces the simulation framework, and lists the configuration for various parameters used in the numerical analysis and the simulation. In section 8.2, the analytical performance results of 802.11p VANETs unicast are compared with the simulated results for both homogeneous traffic and heterogeneous traffic to corroborate the modeling methodologies portrayed in Chapter 3-6. A K-S test is enforced for quantification of the corroboration. Besides, the performance results for the PHY-layer optimization, the MAC-layer optimization and the cross-layer optimization specified in Chapter 7 are also encompassed in Section 8.2.

8.1 The Simulation Configuration

A simulation framework is built on a C++ program to validate the modeling and the optimization of 802.11p VANETs unicast performance. The simulation framework for the modeling and the optimization includes two parts, respectively the traffic simulation and the network simulation.

As for the traffic simulation, there are two scenarios. One scenario is a homogeneous vehicular traffic distribution at various traffic load levels from vehicular density n = 5 cars/km to n = 30 cars/km. The other scenario is the heterogeneous traffic shown in Figure 3.1 with vehicles entering the traffic road at location x = 0 according to the Poisson process at arrival rate 12 cars/min. There is a traffic signaling light located at location x = 2 km which turns red in time interval [4 min, 4.5 min]. During the red light period, from [3], the mean free speed v_f in the front-density-dependent velocity profile (20) follows

$$v_f(x,t) = \begin{cases} v, & x < 1.98 \\ \left(\frac{v}{0.02}\right) * (2 - x), & 1.98 \le x < 2 \\ 0, & 2 \le x < 2.012 \\ \left(\frac{v}{0.02}\right) * (x - 2.012), & 2.012 \le x < 2.032 \\ v, & x \ge 2.032 \end{cases} \tag{83}$$

where v = 1 km/min, a further 0.012 km distance behind the traffic light is allowed for the length of the junction (the speed is zero in the red light duration), and there is additional 0.02 km before and behind the zero-velocity area. In other time, the mean free speed v_f = 1 km/min. In (20), we also assume that Δx = 0.02 km and k_j = 500 cars/km. We run the second traffic scenario simulation for 3000 rounds with different random seeds to obtain the mean vehicular density profile for approximation of the stochastic traffic model (described in Chapter 3).

The network simulation for the single-queue transmission on single channel runs based on the traffic simulation result. We only run 100 simulation rounds for the homogeneous traffic scenario at each density level for respective network performance estimation. For every round of the 3000 traffic simulation trials for the heterogeneous traffic scenario, the vehicular distributions are different with different number of cars in different road units of which each unit is 0.01 km. We run the network simulation for 500 channel intervals for each traffic simulation round to acquire the average delay for one packet transmitted from cars in a unit and the average throughput as follows,

$$\text{Average Delay} = \frac{\sum_{N=1}^{500} time(N)}{\sum_{N=1}^{500} SucNo(N)}, \tag{84}$$

and

$$\text{Average Throughput} = \frac{\sum_{N=1}^{500} SucNo(N)}{\sum_{N=1}^{500} time(N)}, \tag{85}$$

where N denotes each channel interval, $time(N)$ is the total time for packets transmissions and $SucNo(N)$ is the number of packets successfully transmitted in the N-th channel interval. Finally, we can derive the average delay and throughput for the 100 homogeneous traffic simulation rounds at each density level and the 3000 heterogeneous traffic simulation rounds at every location on the traffic route. Table 8.1 lists all the parameters used for the analysis and simulation in this thesis. We set the path-loss exponent α = 2.5 and the SIR requirement β = 10 dB to have $R_I = 2.5R_S$ according to (79). The packet of which the transmission has not finished when the SCH interval expires will be abandoned as there will be newly generated packets in the next SCH interval, which implies that the maximum value of delay for a packet should not be larger than a channel time interval of SCH, i.e., 3125 time slots (50 ms/ 16 μs).

Table 8.1. Parameters used in the analysis and simulation.

Parameter	Value
Transmission range R_S	0.2 km, 0.3 km, 0.4 km, 0.5 km, optimal values in different scenarios
Total number of counter values w	4, 8, 16, 32, optimal values in different scenarios
Density in homogeneous traffic n	5 cars/km, 10 cars/km, 15 cars/km, 20 cars/km, 25 cars/km, 30 cars/km
Arrival rate in heterogeneous traffic	12 cars/min
Traffic light location x	2 km
Red traffic light period	[4 min, 4.5 min]
Path-loss exponent α	2.5
SIR requirement β	10 dB
Maximum doubled times for the initial contention window size m	1
Time slot	16 μs
Packet size	512 bytes
Data rate	6 Mbps
SCH time	50 ms

8.2 Performance Evaluation and Optimization Results of 802.11p VANETs Unicast

For heterogeneous traffic, the vehicular density profile changes as time goes. A snapshot for the mean vehicular density profile $n(x)$ captured at time t = 4.5 min in the road region [0, 4 km] after 3000 heterogeneous traffic simulation rounds is evinced in Figure 8.1. The density keeps at around 12 cars/km at location [0, 1.96 km], drastically jumps to the maximal jamming density 500 cars/km on location [1.96 km, 1.99 km] because there is a huge bunch of vehicles before the red traffic light location x = 2 km, then acutely falls to zero at location 2.02 km behind location 1.99 km, and finally goes up again from location x = 2.45 km behind the zero-density zone by the effect of the traffic light. The vehicular density goes back to approximately 12 cars/km from location 2.53 km until the end of the road region at location 4 km. Some cars exist behind the traffic light in the region (2 km, 2.02 km] are allowed because there is no signal period (red traffic light period) anticipation for drivers. Based on the mean density profile in Figure 8.1, the analytical delay and throughput can be computed, and the simulated results for verifying the analytical model and the optimization can be obtained.

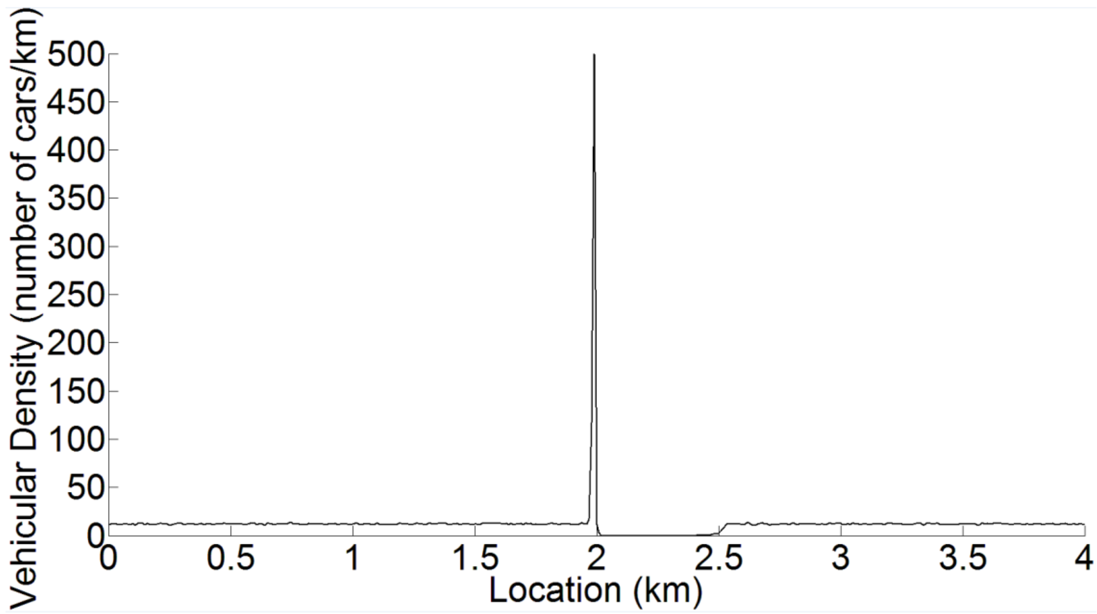

Figure 8.1. The mean vehicular density profile at different locations.

8.2.1 The Results for Performance Modeling

Figure 8.2 plots the analytical and simulated results of delay and throughput in the homogeneous traffic distribution against different vehicular density levels for a single access class queue at four contention window sizes, when transmission range $R_S = 0.2$ km. For the single queue at every one of the four contention window sizes, delay ascends, while throughput descends when density increases as the average contention time of a node for channel access becomes longer and there is higher collision probability for packets transmissions. When the contention window size increases, delay becomes lower and throughput is higher, because there is an exponential back-off procedure in unicast which ensures adequate waiting time for nodes before transmitting and shuns potential collisions for transmissions. However, in broadcasting [6] which lacks the exponential back-off mechanism, the network performance gets worse as the contention window size heightens, as the average contention time for nodes is longer but not long enough for avoidance of collisions. This is one key point that unicast exceeds broadcast. Additionally for unicast as illustrated in Figure 8.3 which adds the simulated results compared with Figure 7.1, when the contention window size increases to an excessively large value, delay will enhance (throughput will drop). All in all, Figure 8.2 reveals that the network performance is strongly affected by different vehicular density with the homogeneous vehicular distribution. The fact that the simulated results match well with the analytical results demonstrates the applicability of the network model in homogeneous traffic.

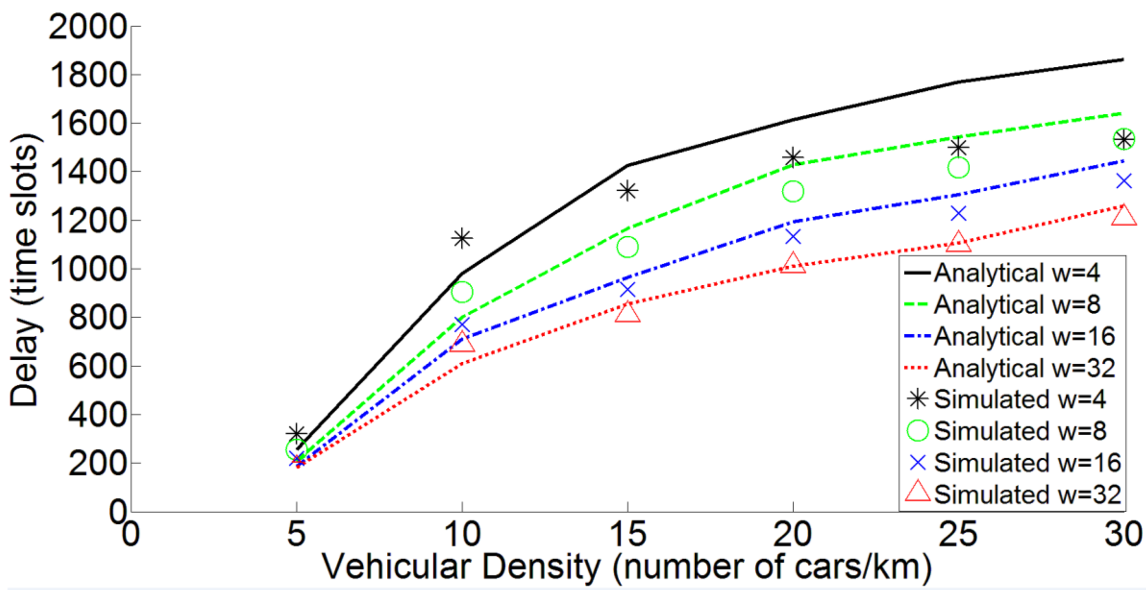

a) Delay

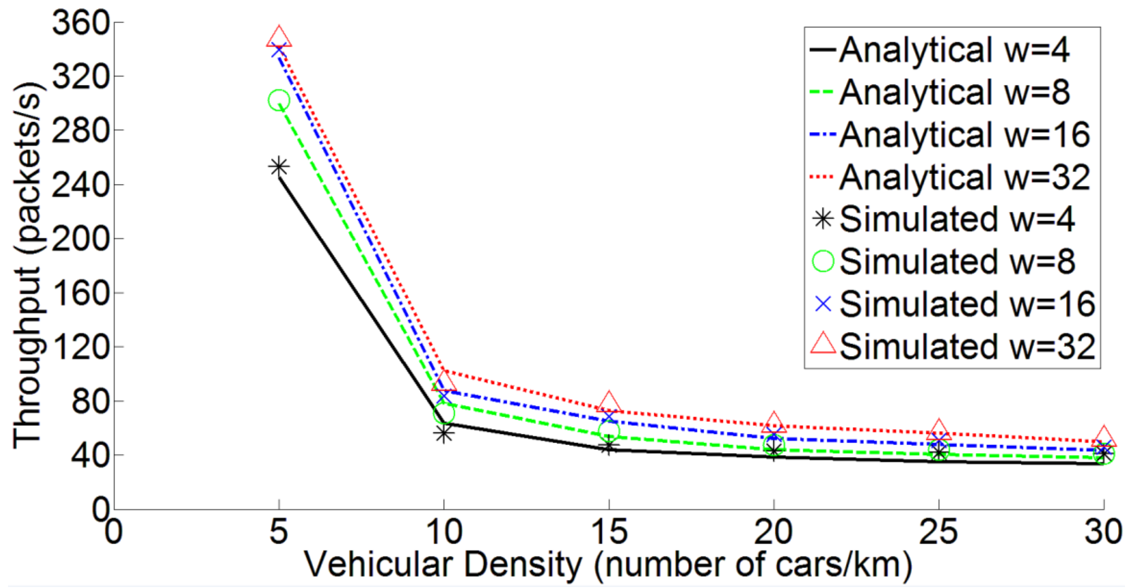

b) Throughput

Figure 8.2. Analytical and simulated performance against the vehicular density for homogeneous traffic.

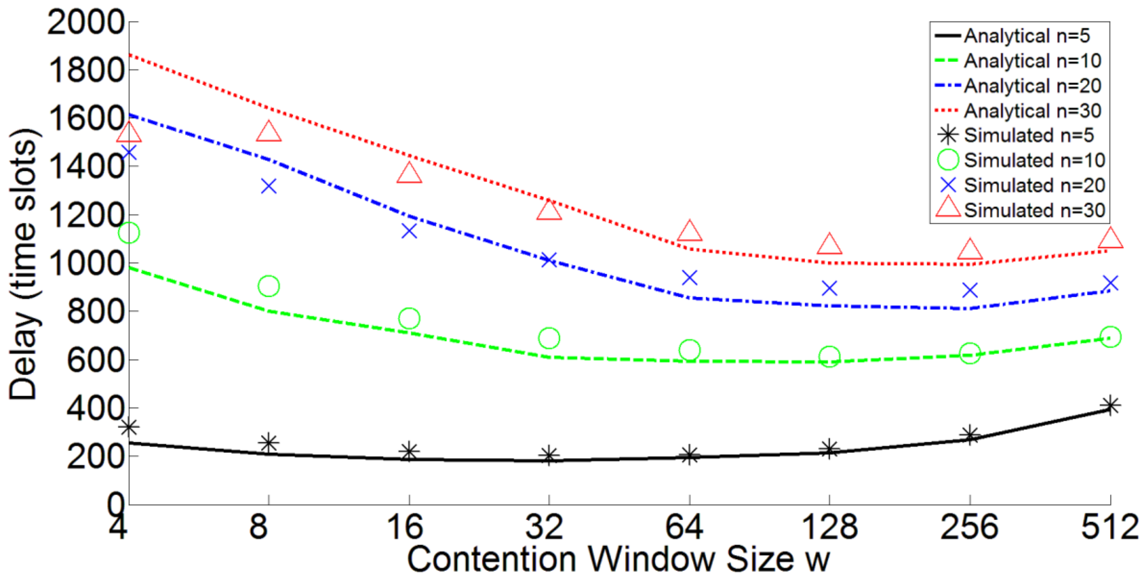

a) Delay

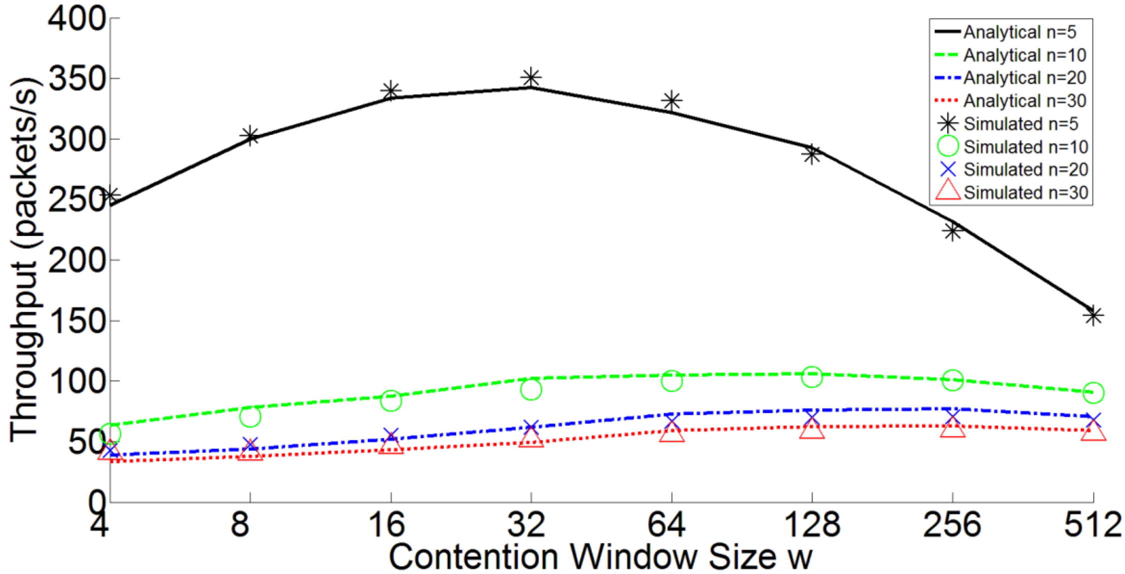

b) Throughput

Figure 8.3. Analytical and simulated performance against the contention window size *w* for homogeneous traffic.

Given the transmission range R_S = 0.2 km (interference range R_I = 0.5 km), Figure 8.4 shows variation of the analytical and simulated delay and throughput for single access class queue with different contention window sizes *w* for the non-homogeneous vehicular density in Figure 8.1 derived from the stochastic traffic model. Delay for a packet transmission for each one of the contention window sizes stays the same in the region [0, 1.46 km] where the traffic distribution is homogeneous with vehicular density of about 12 cars/km. After that, delay starts to rise behind location 1.46 km as there are longer contention time and more collisions engendered by more cars contending for channel access within the forward sensing range 0.5 km beyond location 1.96 km where density begins to increase. Then, the delay reaches the peak at location 1.7 km for *w* = 4 and *w* = 8, at location 1.65 km for *w* = 16, and at location 1.62 km for *w* = 32. But it sharply declines beyond the peak location as there is massive decrement on density in virtue of the zero-density zone after the traffic signal. Behind location 2.5 km, there is a boost of delay as density gradually turns up so that more vehicles exist within the interference range of transmitting cars after the whole zero-density area. Finally, delay rallies to the value approximately equal to delay in [0, 1.46 km] behind location 3.23 km till location 4km as there is a homogeneous vehicular distribution with density of roughly 12 cars/km within the region from location 2.53 km (3.23 km – R_S - R_I) to location 4.5 km in which all the possible hidden nodes are located for the transmitters at locations [3.23 km, 4km]. Similar to Figure 8.2 a), delay is debased by the increasing contention window size. Throughput is inversely proportional to the delay. From this figure, we can assert that the heterogeneous vehicular distribution on a road with the signal control has strong influence on unicast performance, especially the density shockwave in the traffic light area accordingly brings about the delay shockwaves for all the four contention window sizes several hundred meters before the traffic light. Moreover, the availability of the network model based on the stochastic traffic model for heterogeneous traffic is well verified owing to the small deviation between the analytical results and the simulated results. However, the difference is a bit larger at the high contention window size say 32, which purports that our model is more accurate for evaluating the network performance of unicast transmissions with low contention window sizes.

The Kolmogorov-Smirnov test (K-S test) [36, 37] is conducted to inspect the goodness of fit between the analytical results and the simulated results for quantifying the accuracy of our analytical model. The empirical distribution function $F_e(x)$ obtained by the simulated results and the cumulative distribution function $F_c(x)$ obtained by the analytical results are defined as

$$F_e(x) = \frac{1}{n}\sum_{i=1}^{n} I(E_i), \;\; I(E_i) = \begin{cases} 1, & E_i \le x \\ 0, & otherwise \end{cases},$$
$$F_c(x) = \frac{1}{m}\sum_{i=1}^{m} I(C_i), \;\; I(C_i) = \begin{cases} 1, & C_i \le x \\ 0, & otherwise \end{cases}, \tag{86}$$

where n and m denote the number of elements in the simulated result dataset and the analytical result dataset respectively, and E_i is an element of the simulated dataset while C_i is an element of the analytical dataset. Then the K-S statistic is given by the supremum of the set of distances between $F_e(x)$ and $F_c(x)$ as follows,

$$D = sup_x |F_e(x) - F_c(x)|. \tag{87}$$

The results of the K-S test for homogeneous traffic and heterogeneous traffic in Figure 8.2 and Figure 8.4 respectively are presented in Appendix I.

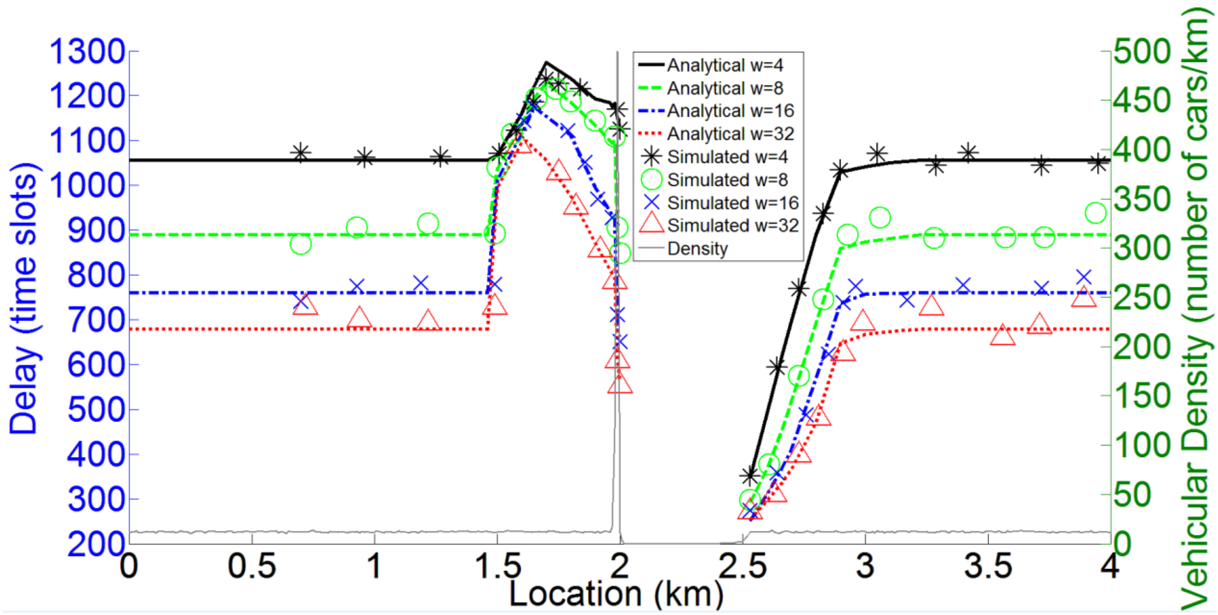

a) Delay

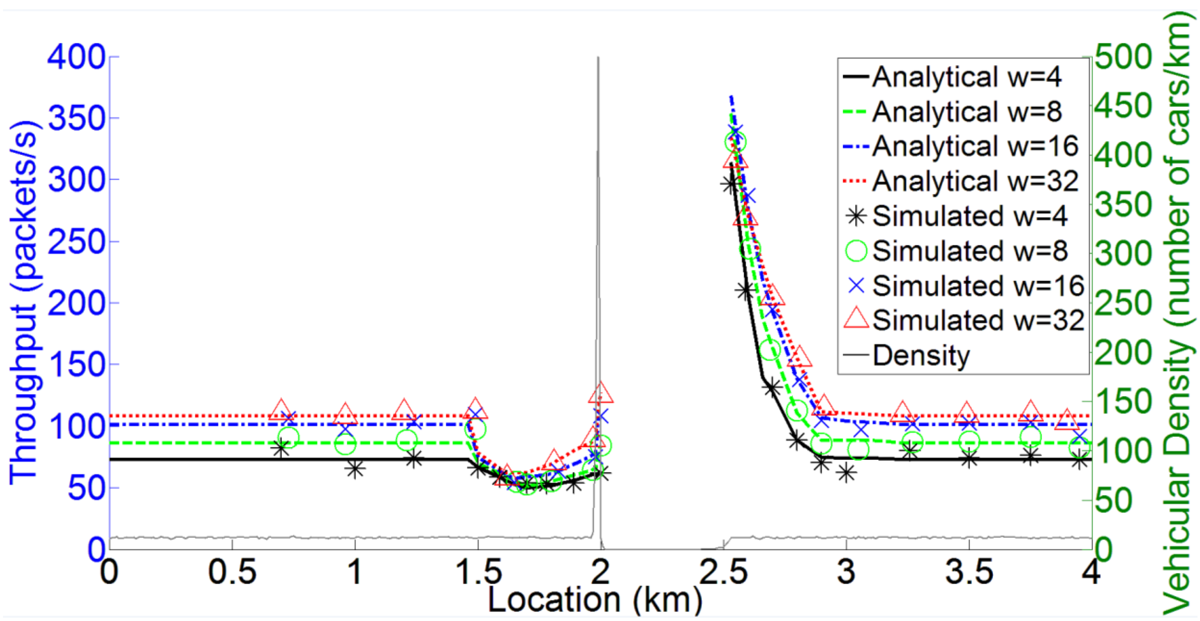

b) Throughput

Figure 8.4. Analytical and simulated performance against the location for heterogeneous traffic.

8.2.2 The Results for Optimizations

With the fixed contention window size $w = 4$, Figure 8.5 and Figure 8.6 manifest the simulated performance results of the PHY-layer optimization for the single access data queue at various vehicular density with the corresponding optimal transmission ranges R_{op} in homogeneous traffic, and the PHY-layer optimization performance results with different optimal transmission ranges by different locations for heterogeneous traffic respectively. The simulated delay and throughput for the PHY-layer optimization is compared by the original performance results with the transmission ranges from 0.2 km to 0.5 km of which each transmission range is invariable for all the density in homogeneous traffic and all the locations in heterogeneous traffic. With the optimal transmission ranges, the delay is lowest and the throughput outperforms the original performance with the fixed transmission ranges. For the homogeneous traffic in Figure 8.5, the optimal delay and throughput almost remains unchanged as density augments, which reflects the robustness of the PHY-layer optimization. What should be noted for the heterogeneous traffic in Figure 8.6 is that there is abnormal soar on optimal delay and slump on optimal throughput near the traffic light at location 2 km, which is extraordinarily dissimilar compared with the original network performance trend. The reason is that there is exceedingly high congestion density in front of the traffic light by which the optimal transmission ranges close to the traffic signal are too small and the corresponding sensing ranges are also very limited, resulting in much more collisions caused by an increasing number of hidden nodes out of the small sensing ranges of the transmitters. Furthermore, it is remarkable that the optimal delay is higher than and the optimal throughput is lower than the original delay and throughput with transmission range 0.2 km respectively around location 2.5 km. For this case, it is because the density there is very low by which the optimal transmission/sensing ranges are relatively large for ensuring the network connection. Cars at that location hence sense more transmitting nodes and endure longer busy time on the channel before packet transmission. However in general, Figure 8.5 and Figure 8.6 verify that the PHY-layer optimization is workable.

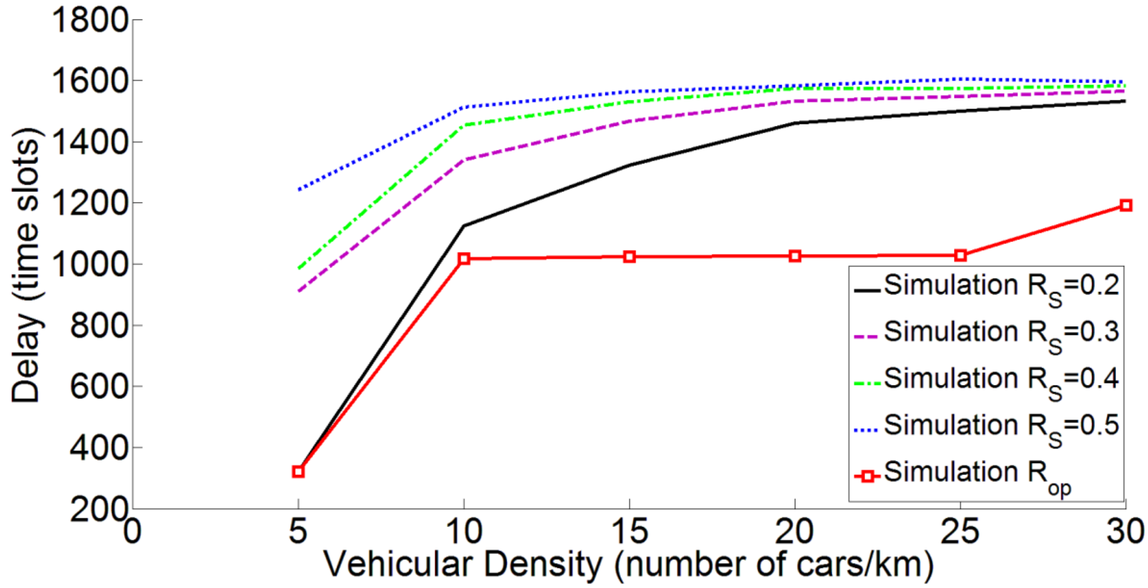

a) Delay

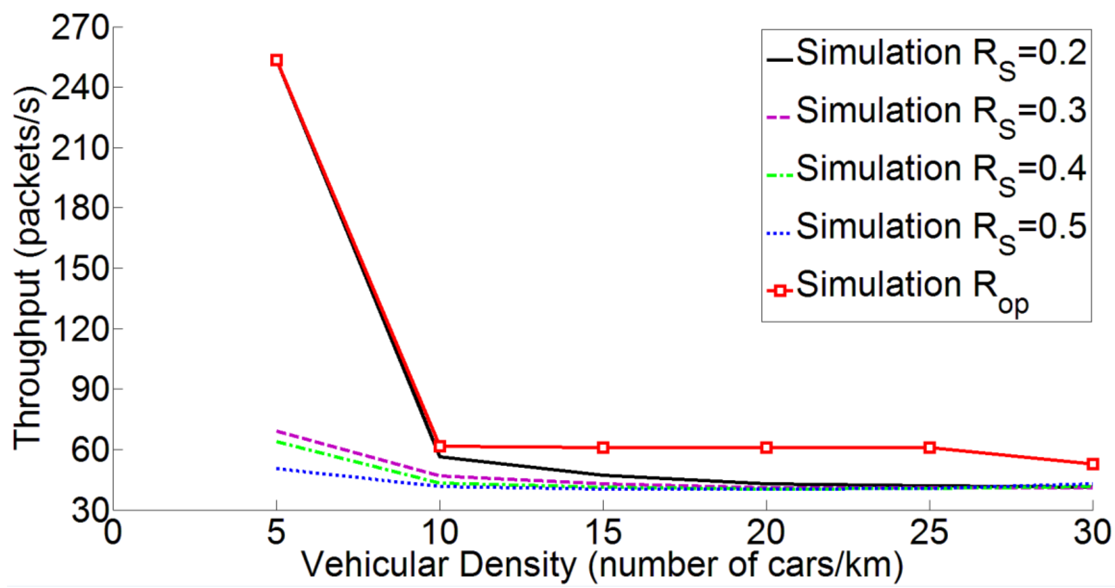

b) Throughput

Figure 8.5. Simulated performance results of the PHY-layer optimization for homogeneous traffic.

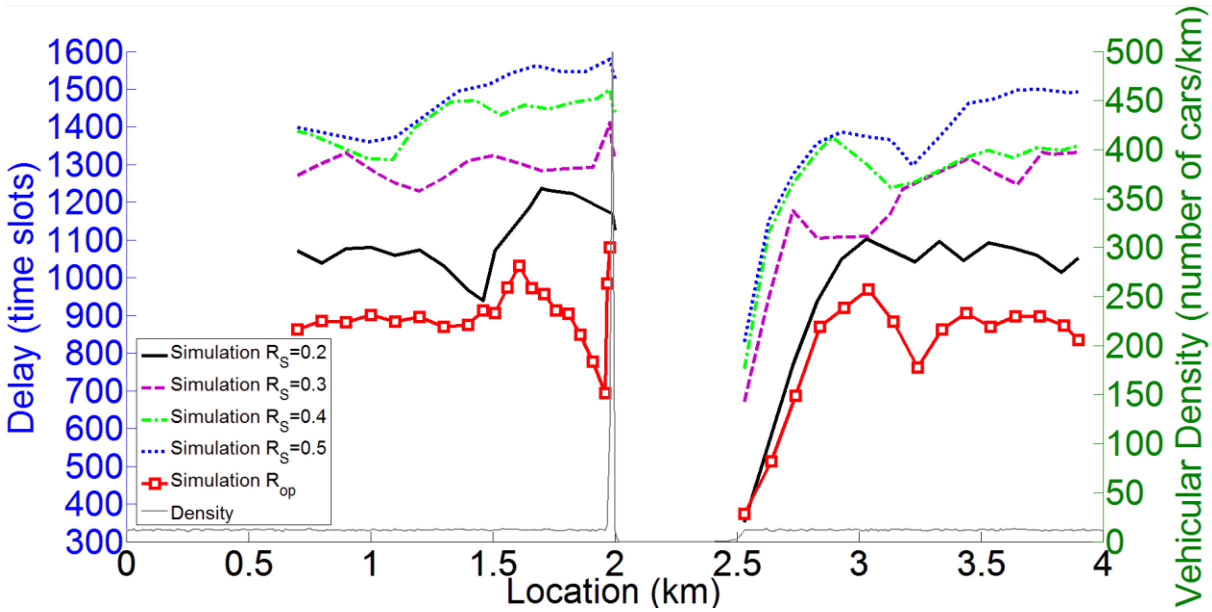

a) Delay

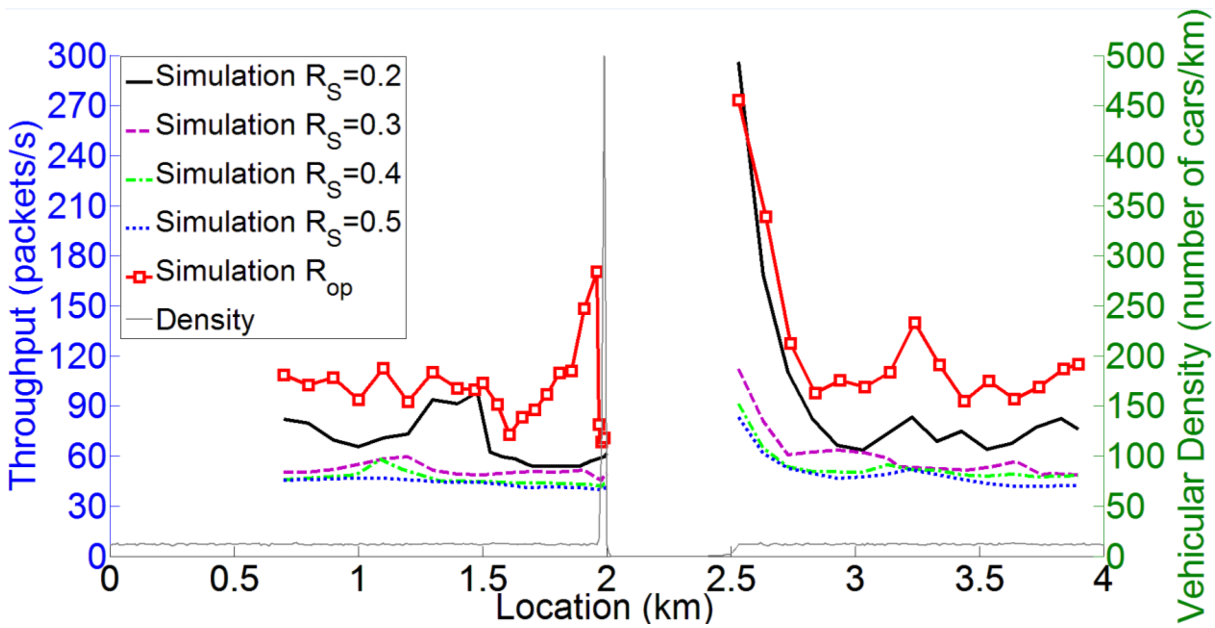

b) Throughput

Figure 8.6. Simulated performance results of the PHY-layer optimization for heterogeneous traffic.

Figure 8.7 and Figure 8.8 display the simulated delay and throughput of the MAC-layer optimization on the single data queue transmission with the optimal contention window sizes w_{op} at different density for homogeneous traffic and every location for non-homogeneous cars distribution, compared with the original network performance with diverse contention window sizes w from 4 to 32. The transmission range for the MAC-layer optimization is fixed to 0.2 km. From the figures, the delay and throughput is optimized, which verifies that the MAC-layer optimization is effective.

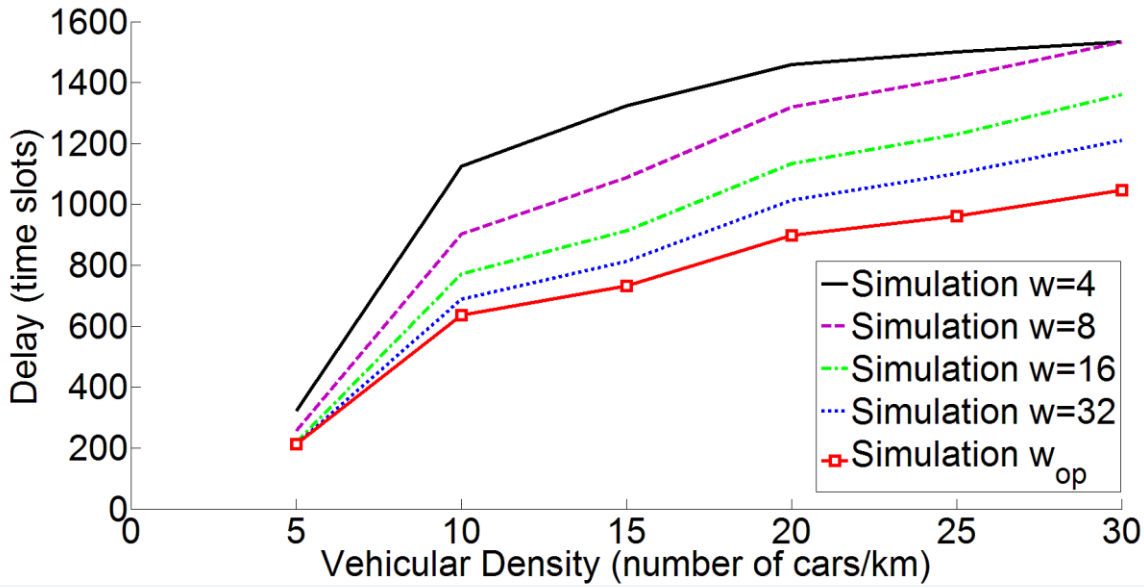

a) Delay

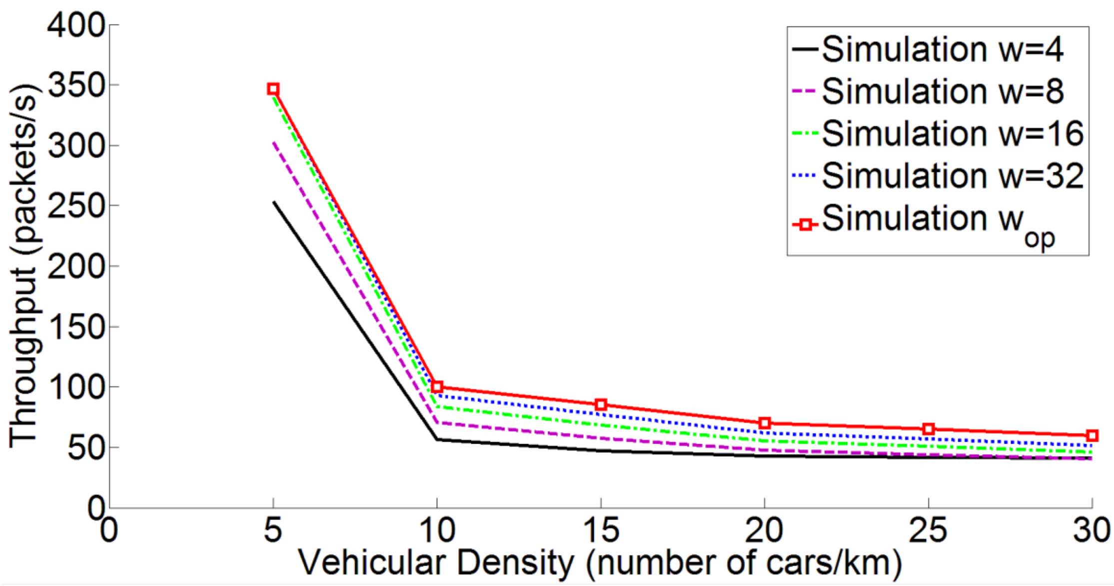

b) Throughput

Figure 8.7. Simulated performance results of the MAC-layer optimization for homogeneous traffic.

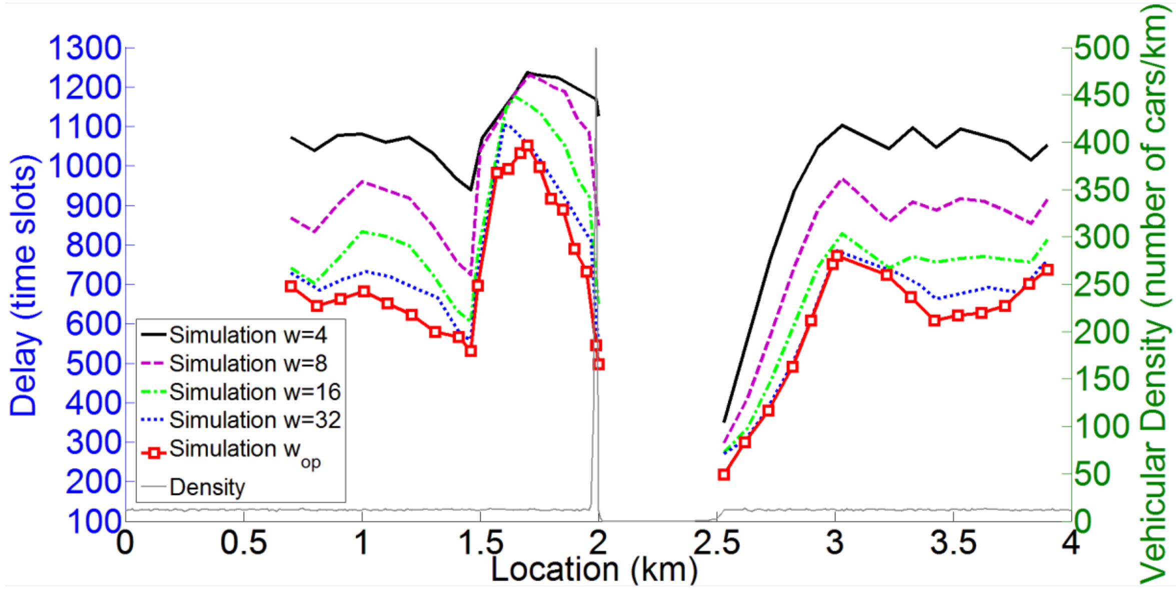

a) Delay

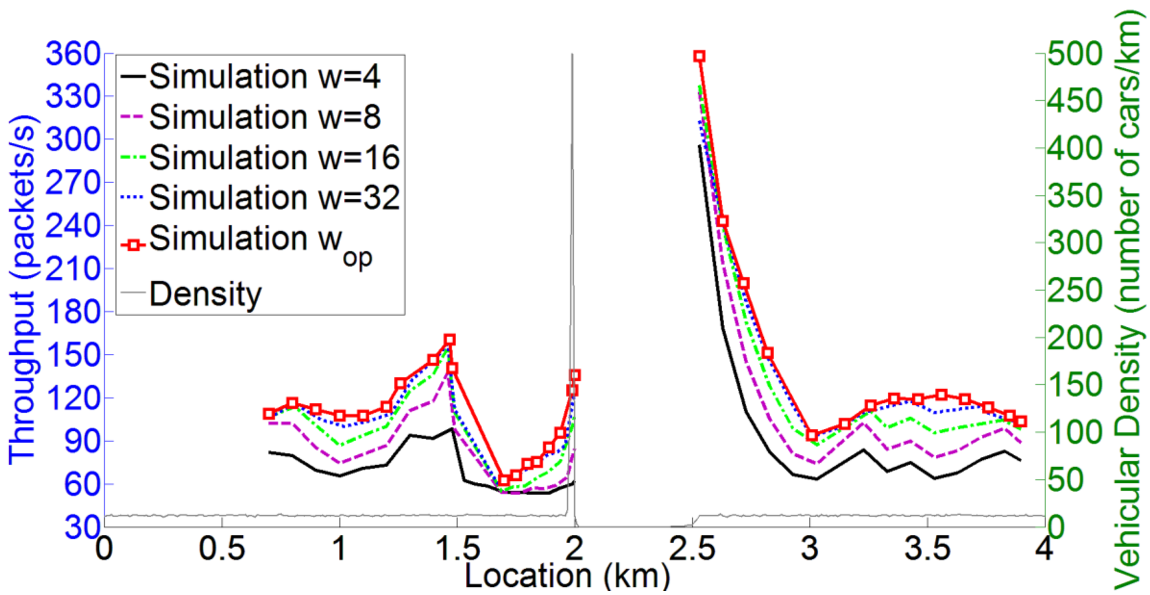

b) Throughput

Figure 8.8. Simulated performance results of the MAC-layer optimization for heterogeneous traffic.

In Figure 8.9 and Figure 8.10, the simulated performance results of the cross-layer optimization for the single access class queue are exhibited together with the original performance results with no optimization (given transmission range R_S = 0.2 km and contention window size w = 4), the PHY-layer optimization performance results and the MAC-layer optimization performance indexes in both homogeneous traffic and heterogeneous traffic. In general, we can observe that the MAC-layer optimization can make higher performance improvement than the PHY-layer optimization. In addition, similar to the PHY-layer optimization, the cross-layer optimization also possesses robustness to nearly freeze deterioration for delay and throughput as the number of vehicles increases in homogeneous traffic as shown in Figure 8.9. In sum, the cross-layer optimization with lowest delay and highest throughput turns out to be superior to the optimization on either the PHY layer or MAC layer.

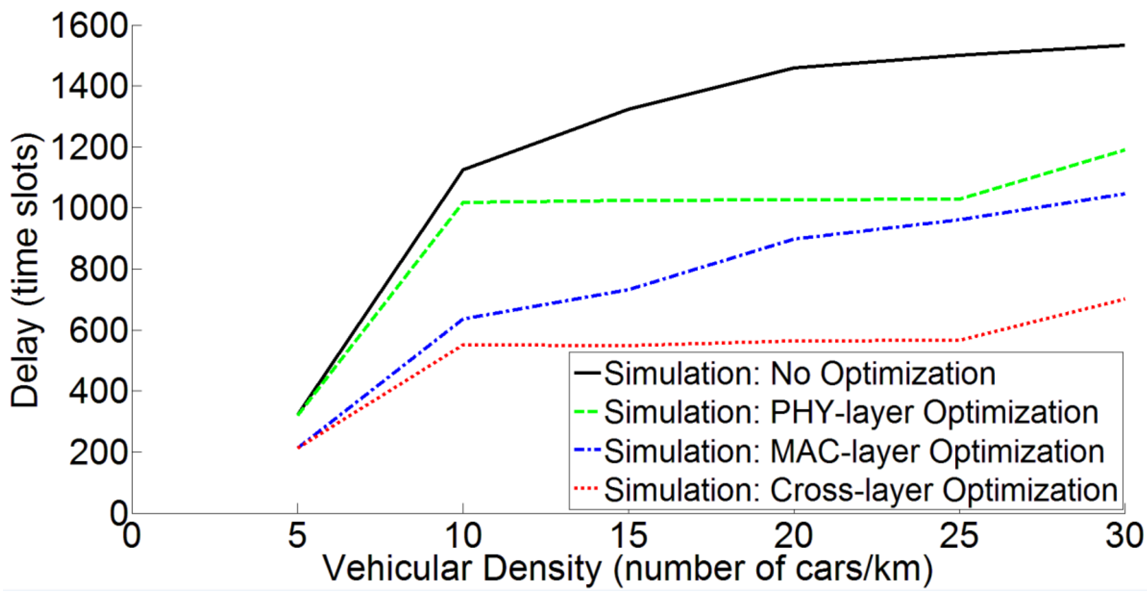

a) Delay

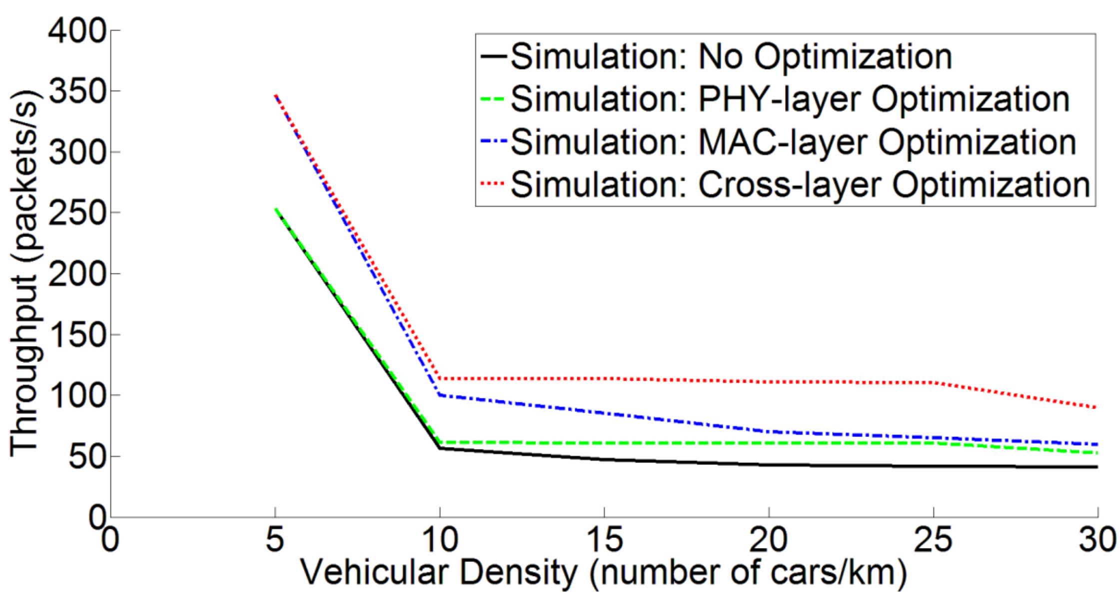

b) Throughput

Figure 8.9. Simulated performance results of the cross-layer optimization for homogeneous traffic.

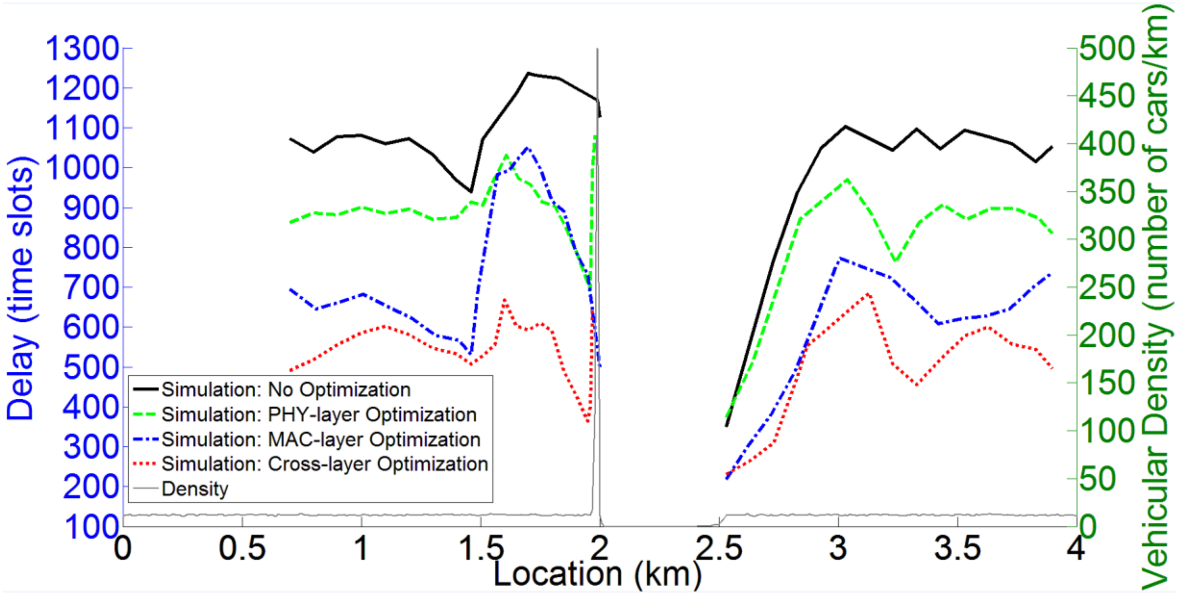

a) Delay

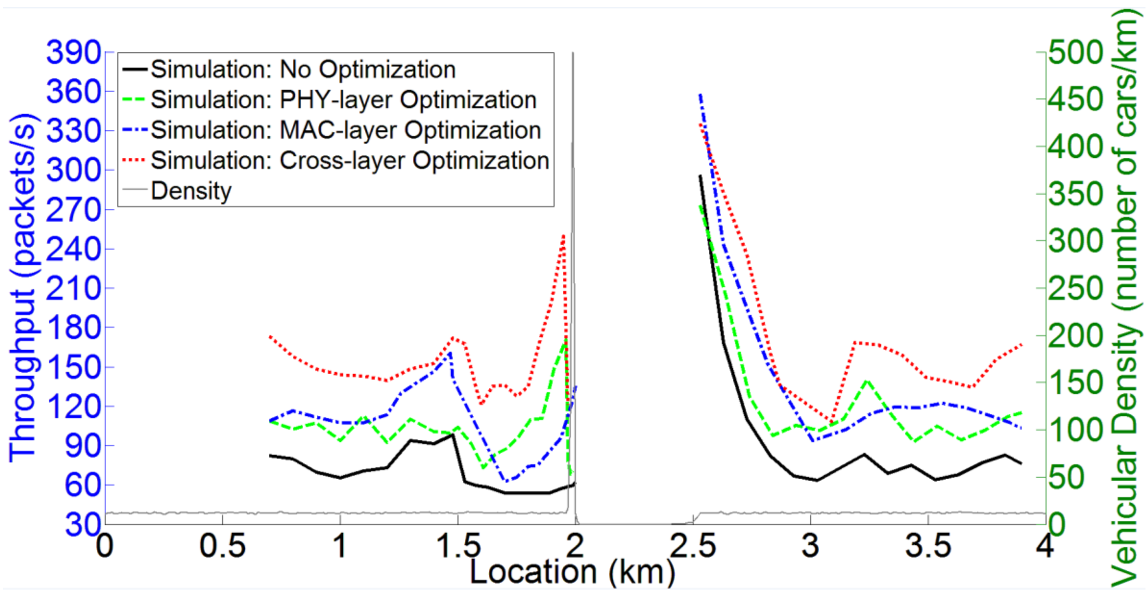

b) Throughput

Figure 8.10. Simulated performance results of the cross-layer optimization for heterogeneous traffic.

As a consequence, delay lowers by averagely around 53% and throughput increases meanly by about 120% with the cross-layer optimization compared with the original performance at transmission range 0.2 km and contention window size 4 for homogeneous traffic. The optimal delay sinks by approximately 45% and the optimal throughput is roughly 104% higher on average with the cross-layer optimization for heterogeneous traffic.

Chapter 9 Conclusions and Discussion

9.1 Conclusions

In this thesis, we firstly mingle the 802.11p VANETs with the practical vehicular traffic to propose a traffic-dynamic-aware network model for performance evaluation of single-AC-queue unicast via the V2V communication mode. The model subsumes a stochastic traffic model and a network model. The former captures characteristics of real-world vehicle motions in the signalized urban traffic, which limns the vehicular density dynamics by a deterministic fluid dynamic model, and portrays the randomness of vehicular traffic through a stochastic model and approximates the vehicular interactions with the effect of traffic lights. For the latter, a 2-D Markov chain based on the stochastic traffic model is exploited to depict the channel access contention for transmissions of a node at a certain location in the network. Then, an interference model is proposed to characterize the effect of collisions on the packets transmitted from the node with respect to the vehicular traffic. By jointly solving the two relationship expressions between the transmission probability and collision probability of the node acquired from the contention model and the interference model, the expected unicast transmission delay and throughput can be readily obtained.

Next, as the modeling methodology can be used to predict vehicular network performance, related network planning can be implemented to achieve higher efficiency of network transmissions and public transportation. In this thesis, the analytical model is further used as the pillar to excogitate cross-layer optimization methods for vehicles at different locations in the network to improve the overall network performance. The cross-layer optimization relies on both the PHY-layer optimization for adjusting the transmission range of each vehicle and the MAC-layer optimization for tuning the contention window sizes of vehicles to the optimal values. The vehicles can directly set the transmission ranges and the contention window sizes to the homologous optimal values which are decided in advance when they move into a particular road region.

The analytical modeling and the optimization are effectively attested by simulation. Given the velocity profile of vehicles as the input, the delay, throughput and the optimized performance with the optimal transmission ranges and contention window sizes can be readily computed according to the set of models and methodologies proposed in this thesis. Our analytical models and the corresponding optimization methods can be used as the prototype for the design and evaluation of other communication protocols in VANETs.

9.2 Limitations

Although simulations well verify the analytical models and the optimization methods, some limitations still exist. In terms of modeling, we have an assumption that the vehicular traffic follows Poisson distribution which has been validated by the empirical data in [3]. But for some scenarios, the traffic of vehicles obeys some other traffic distributions rather than Poisson distribution. For example, Zhang [46] demonstrated that the lane-level traffic in Shanghai followed Gaussian distribution and the traffic in each road segment was no longer independent. Therefore, other traffic distributions should also be taken into consideration for more accurate traffic modeling. Furthermore, our traffic model only involves the 1-D road scenario which is unable to encompass all traffic factors. Hence, the two-dimensional traffic road with more complicated road topologies including multiple directions and lanes, curvatures and gradients should be extended by superposing multiple signalized 1-D road segments. The burst traffic causing sudden topology changes should also be handled in further traffic model. Moreover, multi-channel transmissions with multiple access classes should be modeled to overcome the shortage that there is only single AC queue transmitted on single channel considered. This thesis assumes that the packet transmission fails solely because of collisions, however there are other factors that cause transmission failures such as channel coding errors, loss of packets, bit errors and fading which should also be introduced into the 802.11p unicast realm. Finally, only constant-length packets are assumed to be transmitted, packets with variable lengths should be considered in future work.

With regards to the optimization, we only focus on transmission range adjustment on the PHY layer and contention window size tune on the MAC layer. Actually for the PHY-layer optimization, the signaling optimization on the road can be carried out for a more efficient traffic. Adaptive data rate can also be set to increase throughput. Hidden nodes can be withstood by carrier-sensing range adjustments. The energy consumption reduction should also be evaluated. For the MAC-layer optimization, as the performance curves showed in Figure 7.1 are analytically unimodal, other standard searching methods such as golden section search [47] can also be explored to more efficiently identify the optimal contention window size. AIFS can also be adjusted like [23] which implements AIFS segregation. Adjustment of the maximum number of times m for the initial contention window size to be doubled and the maximum number of retransmissions f after stage m and before the packet is discarded should also be studied. In addition, the CCH/ SCH interval can be adjusted based on Markov modeling [32, 12].

9.3 Future Works

The future works related to 802.11p VANETs modeling and optimization primarily includes five items beneath:

1. The V2I communication and the relevant optimization with rational deployment of infrastructures ought to be analyzed to build a comprehensive analytical model of VANETs performance together with the V2V model in this thesis. For V2I communications, the vehicular distribution is still uneven and the workloads on different infrastructures are lopsided. We can refer to the novel V2I hybrid optimization method named Dynamic Resources Allocation Scheme (DRAS) proposed in [38] which regarded moving buses being regularly distributed as mobile relay infrastructures to offload some burden from infrastructure nodes for providing better network performance.
2. Routing is another vital topic in vehicular networks. There are topology-based routing protocols [39]: DSDV, OLSR, AODV, and DSR. These protocols route packets based on exchanged link information, which might not be accommodated

for the highly dynamic vehicular environments with frequent transformation of the network topology. There are also position-based routing protocols for VANETs, such as GPSR [40] and GRANT [41] which determine the route based on the geographic location of neighboring nodes with greater promise. We can investigate the performance of existing routing protocols in VANETs and decide the proper one to be used for different density levels. As routing protocols are fundamental for Quality of Service (QoS) enhancement, the optimization for routing protocols should be brought to the forefront. For example, a reactive routing protocol with a dynamic allocation scheme of the available multi-frequency spectrum proposed in [42] for optimizing the lengths of paths (hop-count), co-channel noise and link reliability can also be availed as an optimized routing protocol based on our analytical models. We can also take advantage of routing protocols for the optimization of vehicular networks such as recovering broken links through cross-layer-based real-time local repair (RTLR) approaches [43].

3. We can apply cooperative communications on VANETs for promoting reliability of transmission links. As an illustration, [44] proposed the cooperative ad-hoc MAC (CAH-MAC) protocol in which vicinal nodes cooperate in retransmitting packets failed in the previous transmission due to poor channel condition. The cooperation implemented in unreserved time slots could mitigate the dissipation of time slots, enhance network throughput, and debase the packet dropping rate. Whereas the CAH-MAC reserved the consideration of relative node mobility which can be incorporated into our analytical models with the dynamic network topology.
4. The software defined network (SDN) can be utilized in VANETs. The conventional homogeneous vehicular communication based on cellular networks and 802.11p VANETs is unable to meet the requirement of burgeoning vehicular network applications with heterogeneous resources which however can be more efficiently managed by SDN with unified abstraction.
5. VANETs can be exploited for traffic accident risk management to reduce casualty. For example, [45] proposed a system in which vehicles adjusted their risk

estimate levels based on the risk values received from their neighbors in the VANET. The system can be coupled with our model as well.

Appendix I The K-S Test Results

In this appendix, the K-S test results for comparing the analytical and simulated performance in both the homogeneous traffic and heterogeneous traffic are computed through the expressions (86) and (87) at a significance level of 0.05. $h = 0$ and p-value is greater than the significance level if the null hypothesis cannot be rejected, and $h = 1$ otherwise. The K-S test results with h value and p-value for the homogeneous traffic in Figure 8.2 are tabulated in Table I.1, and the results for the heterogeneous traffic in Figure 8.4 are listed in Table I.2 and Table I.3.

Table I.1. K-S test results for analytical and simulated delay and throughput in homogeneous traffic.

	***w* = 4**	***w* = 8**	***w* = 16**	***w* = 32**	**Row-wise average value**
K-S result	0.5	0.33	0.17	0.17	0.29
h	0	0	0	0	0
***p*-value**	0.32	0.81	0.99	0.99	0.78

Table I.2. K-S test results for analytical and simulated delay in heterogeneous traffic.

	***w* = 4**	***w* = 8**	***w* = 16**	***w* = 32**	**Row-wise average value**
K-S result	0.24	0.22	0.27	0.33	0.27
h	0	0	0	0	0
***p*-value**	0.53	0.59	0.33	0.15	0.4

Table I.3. K-S test results for analytical and simulated throughput in heterogeneous traffic.

	***w* = 4**	***w* = 8**	***w* = 16**	***w* = 32**	**Row-wise average value**
K-S result	0.21	0.21	0.28	0.35	0.26
h	0	0	0	0	0
***p*-value**	0.74	0.74	0.43	0.19	0.53

Bibliography

[1] H. J. F. Qiu, I. W.-H. Ho, and C. K. Tse, "A stochastic traffic modeling approach for 802.11p VANET broadcasting performance evaluation," *IEEE International Symposium on Personal Indoor and Mobile Radio Communications (PIMRC)*, 2012.

[2] N. S. Nafi and J. Y. Khan, "A VANET based intelligent road traffic signalling system," *Australasian Telecommunication Networks and Applications Conference (ATNAC)*, 2012.

[3] I. W.-H. Ho, K. K. Leung, and J. W. Polak, "Stochastic model and connectivity dynamics for VANETs in signalized road systems," *IEEE/ACM Transactions on Networking*, vol. 19, no. 1, pp. 195-208, 2011.

[4] X. Ma and X. Chen, "Delay and broadcast reception rates of highway safety applications in vehicular ad hoc networks," *Mobile Networking for Vehicular Environments*, 2007.

[5] "Wireless LAN Medium Access Control (MAC) and the Physical Layer (PHY) Specifications, Amendment 6: Wireless Access in Vehicular Environment," IEEE Std. 802.11p, 2010.

[6] H. J. Qiu, I. W.-H. Ho, C. K. Tse, and Y. Xie, "A Methodology for Studying 802.11p VANET Broadcasting Performance with Practical Vehicle Distribution," *IEEE Transactions on Vehicular Technology*, vol. 64, no. 10, pp. 4756 – 4769, 2015.

[7] O. Chakroun, S. Cherkaoui, and J. Rezgui, "MUDDS: Multi-Metric Unicast Data Dissemination Scheme for 802.11p VANETs," *Wireless Communications and Mobile Computing Conference (IWCMC)*, 2012.

[8] H. Menouar, R. Aissaoui, F. Filali, A. Abu-Dayya, and A. Belghith, "Cellular-based location service to support GeoUnicast communications in vehicular wireless networks," *International Conference on Telecommunications (ICT)*, 2013.

[9] T. Umer, Z. Ding, B. Honary and H. Ahmad, "Implementation of microscopic parameters for density estimation of heterogeneous traffic flow for VANET," *International Symposium on Communication Systems Networks and Digital Signal Processing (CSNDSP)*, 2010.

[10] G. Bianchi, “Performance analysis of the IEEE 802.11 distributed coordination function,” *IEEE Journal on Selected Areas in Communications*, vol. 18, no. 3, pp. 535 – 547, 2000.

[11] C. Han, M. Dianati, R. Tafazolli, R. Kernchen, and Sherman X. Shen, “Analytical study of the IEEE 802.11p MAC sublayer in vehicular networks,” *IEEE Transactions on Intelligent Transportation Systems*, vol. 13, no. 2, pp. 873 – 886, 2012.

[12] Q. Wang, S. Leng, H. Fu, Y. Zhang, and H. Weerasinghe, “An enhanced multi-channel MAC for the IEEE 1609.4 based vehicular ad hoc networks,” *INFOCOM IEEE Conference on Computer Communications Workshops*, 2010.

[13] “IEEE Standard for Wireless Access in Vehicular Environments (WAVE)—Multi-channel Operation,” IEEE Std. 1609.4, 2010.

[14] G. V. Rossi and K. K. Leung, “Performance Tradeoffs by Power Control in Wireless Ad-Hoc Networks,” *International Wireless Communications and Mobile Computing Conference (IWCMC)*, 2013.

[15] X. Guan, R. Sengupta, H. Krishnan, and F. Bai, “A Feedback-Based Power Control Algorithm Design for VANET,” *Mobile Networking for Vehicular Environments*, 2007.

[16] J. Tian and C. Lv, “Connectivity Based Transmit Power Control in VANET,” *International Wireless Communications and Mobile Computing Conference (IWCMC)*, 2012.

[17] X. Ma, J. Zhang, X. Yin and K. Trivedi, “Design and Analysis of a Robust Broadcast Scheme for VANET Safety-Related Services,” *IEEE Transactions on Vehicular Technology*, vol. 61, no. 1, pp. 46-61, 2012.

[18] S. Sharafkandi, G. Bansal, J. B. Kenney and D. H. C. Du, “Using EDCA to improve vehicle safety messaging,” *Vehicular Networking Conference (VNC)*, 2012.

[19] K. Bilstrup, E. Uhlemann, E. Strom and U. Bilstrup, “Evaluation of the IEEE 802.11p MAC Method for Vehicle-to-Vehicle Communication,” *IEEE Vehicular Technology Conference (VTC)*, 2008.

[20] H. J. F. Qiu, I. W.-H. Ho, C. K. Tse, and Y. Xie, “Technical Report: A Methodology for Studying

802.11p VANET Broadcasting Performance with Practical Vehicle Distribution," arXiv: 1410.3978, 2014.

[21] X. Shen, R. Zhang, X. Cheng, Y. Yang and B. Jiao, "Distributed multi-priority congestion control approach for IEEE 802.11p vehicular networks," *International Conference on ITS Telecommunications (ITST)*, 2012.

[22] C. W. Hsu, C. H. Hsu and H. R. Tseng, "MAC Channel Congestion Control Mechanism in IEEE 802.11p/WAVE Vehicle Networks," *Vehicular Technology Conference (VTC)*, 2011.

[23] I. Koukoutsidis and V. A. Siris, "802.11e EDCA Protocol Parameterization: A Modeling and Optimization Study," *IEEE International Symposium on World of Wireless, Mobile and Multimedia Networks (WoWMoM)*, 2007.

[24] G. V. Rossi, K. K. Leung and A. Gkelias, "Density-based optimal transmission for throughput enhancement in vehicular ad-hoc networks," *International Conference on Communications (ICC)*, 2015.

[25] P. Patras, A. Banchs and P. Serrano, "A control theoretic approach for throughput optimization in IEEE 802.11e EDCA WLANs," *Mobile Networks and Applications (MONET)*, 2008.

[26] S. Wang, A. Song, J. Wei and A. Hafid, "Maximizing Saturation Throughput of Control Channel in Vehicular Networks," *International Conference on Mobile Ad-hoc and Sensor Networks (MSN)*, 2011.

[27] Y. Xie, I. W.-H. Ho and L. F. Xie, "Stochastic modeling and analysis of unicast performance in 802.11p VANETs," *International Conference on Information, Communications and Signal Processing (ICICS)*, 2015.

[28] "NS3 VANET Projects", http://ns3-code.com/ns3-vanet-projects/.

[29] P. Gomes, F. Vieira and M. Ferreira, "Sustainable Highways with Shadow Tolls based on VANET Advertising," *ACM international workshop on Vehicular inter-networking, systems, and applications*, 2013.

[30] "Wireless LAN Medium Access Control (MAC) and Physical Layer (PHY) Specifications Amendment 8: Medium Access Control (MAC) Quality of Service Enhancements," IEEE Std.

802.11e, 2005.

[31] D. Jiang and L. Delgrossi, "IEEE 802.11p: Towards an International Standard for Wireless Access in Vehicular Environments," *IEEE Vehicular Technology Conference (VTC Spring)*, 2008.

[32] J. Miˇsi´c, G. Badawy, S. Rashwand and V. B. Miˇsi´c, "Tradeoff issues for CCH/SCH duty cycle for IEEE 802.11p single channel devices," *Global Telecommunications Conference (GLOBECOM)*, 2010.

[33] "Omnidirectional antenna", https://en.wikipedia.org/wiki/Omnidirectional_antenna.

[34] "Directional antenna", https://en.wikipedia.org/wiki/Directional_antenna.

[35] I. W.-H. Ho, K. K. Leung and J. W. Polak, "Optimal Transmission Probabilities in VANETs with Inhomogeneous Node Distribution," *IEEE International Symposium on Personal, Indoor and Mobile Radio Communications (PIMRC)*, 2009.

[36] "Kolmogorov-Smirnov Test," http://www.physics.csbsju.edu/stats/KS-test.html.

[37] "Kolmogorov–Smirnov test", https://en.wikipedia.org/wiki/Kolmogorov%E2%80%93Smirnov_test.

[38] T. Jiang, Y. Alfadhl and K. K. Chai, "Efficient Dynamic Scheduling Scheme between Vehicles and Roadside Units based on IEEE 802.11p/WAVE Communication Standard," *International Conference on ITS Telecommunications (ITST)*, 2011.

[39] K. C. Lee, U. Lee, and M. Gerla, "Survey of Routing Protocols in Vehicular Ad Hoc Networks," *Advances in Vehicular Ad-hoc Networks*, pp. 149 – 170, 2010.

[40] B. Karp and H. T. Kung, "GPSR: greedy perimeter stateless routing for wireless networks," *International Conference on Mobile computing and Networking (MobiCom)*, 2000.

[41] S. Schnaufer and W. Effelsberg, "Position-based unicast routing for city scenarios," *International Symposium on a World of Wireless, Mobile and Multimedia Networks (WoWMoM)*, 2008.

[42] C. Sottile, A. F. Santamaria and S. Marano, "A Reactive Routing Protocol for VANETs Based on Composite Metric Concept," *International Symposium on Performance Evaluation of Computer*

and Telecommunication Systems (SPECTS), 2014.

[43] B-J Chang, Y-H Liang, J-T Lai, and J-W Wang, "Cross-Layer-based Real-Time Local Repair for Multicasting in Distributed Vehicular Ad-hoc Networks," *World Telecommunications Congress (WTC)*, 2012.

[44] S. Bharatit and W. Zhuang, "Performance Analysis of Cooperative ADHOC MAC for Vehicular Networks," *Global Communications Conference (GLOBECOM)*, 2012.

[45] E. Fitzgerald and B. Landfeldt, "System for Coupled Road Traffic Utility Maximisation and Risk Management Using VANET," *International IEEE Conference on Intelligent Transportation Systems (ITSC)*, 2012.

[46] W. Zhang, Y. Yang, H.Qian, Y. Zhang, M. Jiao and T. Yang, "Macroscopic traffic flow models for Shanghai," *IEEE International Conference on Communications (ICC)*, 2012.

[47] "Golden section search", https://en.wikipedia.org/wiki/Golden_section_search.